Master Thesis

Examination of grey matter volume in hippocampus subregions across diagnosis phenotypes of the Alzheimer's Disease Neuroimaging Initiative (ADNI)

Written by: Ahmed Abdelghafar, master student of translational neurosciences, university of Düsseldorf.

Supervised by: Anna Plachti and Dr. Shahrzad Kharabian, Institute of Neuroscience and Medicine - 7 (INM7), Forschungszentrum Jülich (FZJ).

Summary

Alzheimer's Disease (AD) constitutes a step-wise structural and functional deterioration of some brain structures such as the hippocampus. Hippocampus atrophy, detected by structural MRI, is considered one of the AD's markers, mentioned in the new AD diagnostic criteria by Dubois and colleagues in 2007. In previous studies, it was proposed that a possible dissimilar hippocampus grey matter subregional atrophy occurs along AD progression.

In this project we were trying to investigate the differential hippocampus subregional mean Grey Matter Volume (GMV) affection in different diagnosis phenotypes of AD. Our subjects' data were obtained from the Alzheimer's Disease Neuroimaging Initiative (ADNI) database, divided according to the each subject probable diagnosis into 5 diagnosis groups representing different stages, starting from normal controls until a probable AD. Our hippocampus model was adapted from the work done by Plachti and colleagues in 2019, who parcellated the hippocampus into 3 clusters on each side based on multimodal Connectivity Based Parcellation (CBP). In this project, the mean GMV in subjects' T1-weighted, 3T structural MRI images, present on ADNI database, using Voxel Based Morphometry (VBM) was assessed, after employing a series of images' post-acquisition quality control steps. The results suggested that there was a differential hippocampus GMV atrophy in different subregions in various stages of AD. The Atrophy severity was possibly increasing with more advanced stages towards probable AD stage. Moreover, atrophy has been found dependent on the diagnostic stage on the right hippocampus. The most affected subregions by different stages of the disease on both hemispheres were the right, left intermediate and left posterior clusters. This study further bolsters some of similar previous studies, done on different hippocampus models, comparing hippocampus volumes along its longitudinal axis in different AD stage, which had similar results as ours. Moreover it opens the door towards further research of the most affected parts in each subregion, by using a hippocampus model with higher number of partitions along the anterior-posterior axis i.e. 7 to know more specifically where the volume change took place.

Introduction

Alzheimer's Disease

Alzheimer's Disease (AD) is a neurodegenerative disease, characterized by a gradually developing brain pathology, which probably starts years to decades before the development of its clinical manifestations (McKhann et al., 1984; Peterson et al., 2009; Weiner et al., 2013). AD pathology starts with a serious of pathological microstructural changes namely Beta amyloid plaques and tau neurofibrillary tangles deposition combined with neuronal degeneration and synapse loss followed by structural brain changes including brain atrophy, as described in (Jack et al., 2008; 2009; Shaw, 2008; Weiner et al., 2013). These pathological changes are possibly correlated with the clinical manifestations, occurring in the disease, primarily in the form of dementia, which includes progressive memory decline as well as other cognitive functions, possibly accompanied by language disturbance and behavioral changes, disturbing daily-living activities (McKhann et al., 1984).

Alzheimer's disease diagnosis phenotypes.

Alzheimer's disease diagnosis phenotypes represent different stages of the disease along its progression including non-demented groups, having subjective memory affection and/or objective memory concern, measured by neuropsychological tests and a demented group which is the clinical probable AD. A lot of methods could be employed which aid in classifying these diagnostic stages.

The consortium of the National Institute of Neurological and Communicative Disorders and Stroke (NINCDS) and the Alzheimer's Disease and Related Disorders Association (ADRDA), established in 1984 (McKhann et al., 1984), represents one of the earliest attempts to set unified criteria for AD diagnosis groups classification, which viewed AD as a ''clinical-pathological entity'' (Jack et al. 2011), employing serious of clinical, neuropsychological, laboratory and imaging methods for AD diagnosis and classification. To evaluate the clinical

aspect of a ''Probable AD'', some neuropsychological tests such as Mini Mental State Examination (MMSE) are used. Imaging techniques such as EEG, CT, MRI and PET, as well as some laboratory tests possibly detect the pathological aspect. 'Definite AD' diagnosis is based on histopathological proof acquired from biopsy or autopsy.

Our study's cohort is adapted from the Alzheimer's Disease Neuroimaging Initiatve (ADNI), which employed the NINCDS-ASRDA criteria as a method for differentiation of the demented AD group from the other 4 non-demented diagnosis groups (Cognitive Normal (CN), Subjective Memory
Concern (SMC), Early Mild Cognitive Impairment (EMCI) and Late Mild Cognitive Impairment (LMCI), included in our study. In ADNI, AD group represents the clinical probable AD in NINCDS-ASRDA criteria. In this study all the 5 groups were included.

Mild Cognitive Impairment (MCI) is a preliminary stage before AD, in which subjects suffer from cognitive problems, however they don't meet the NINCDS-ADRDA criteria for clinical probable AD (Khan et al., 2016; Peterson et al., 1999; 2001), in another words they are not demented and can perform their daily life activities. MCI subjects were found to be more deteriorating towards dementia than the normal aging i.e. CN subjects in terms of cognitive functions (Flicker, Ferris, & Reisberg, 1991; Peterson et al., 2001) and were even described as being in a ''transitional stage'' between healthy aging and AD (Peterson et al., 2001). MCI subjects, in general, are believed to have a bigger chance to develop AD with a yearly rate of 10% to 12% per year (Peterson et al., 1999) or even 10% to 25% per year (Grand, Caspar & Macdonald, 2011) compared to normal controls with 1% to 2% per year (Peterson et al., 1999). MCI subjects are divided to EMCI and LMCI groups in ADNI according to their memory functions assessed by their performance in the Wechsler memory scale test – delayed recall. EMCI and LMCI have shown a rate of conversion of 10.8% and 24.9% respectively to AD dementia in a 6 years study (Jessen et al., 2014).

Subjective Memory Concern (SMC) is a subjective report of memory affection

from the subject or his close contact without any objective, quantified cognitive affection. Some studies have reported a possible risk for SMC subjects to develop AD dementia (Jessen, 2010; Reisberg, Shulman, Torossian, Leng & Zhu, 2010). SMC subjects have shown a rate of conversion of 6.2% to AD dementia less than that of EMCI and LMCI subjects (Jessen et al., 2014). In a review study SMC subjects showed 1.5-3 times higher conversion rate to MCI or AD than the normal elderly controls (Mendonça, Alves, & Bugalho, 2015).

Structural brain changes, an important maker of Alzheimer's disease.

Structural brain changes could help in early detection of a probable AD (Dubois et al., 2007; McKhann et al., 2011). Different imaging techniques like structural, functional MRI (sMRI, fMRI) as well as Positron Emission Tomography (PET) could be employed in giving a possibility to detect such structural as well as some functional changes taking place in AD, as hippocampal atrophy using sMRI, neural networks abnormalities with fMRI and amyloid plaques deposition with PET. The National Institute of Aging and Alzheimer's Association (NIA-AA) (Jack et al., 2011; McKhann et al., 2011; Sperling 2011) as well as the International Working Group (IWG) (Dubois et al., 2007; 2010; 2014) represent recent initiatives, which aimed at incorporating imaging markers, as a possible way to track and early suspect AD through detecting the structural changes occurring in AD brains.

sMRI is a non-invasive method, which helped in the in vivo detection of AD's structural brain changes as well as their quantification in the absence of any radiation exposure. sMRI, aided to detect changes in Grey Matter Volume (GMV) (Guo et al., 2014) and White Matter Volume (WMV) in AD (Guo et al., 2010), where the GMV loss reflects brain morphometric changes with regards to neuronal microstructure including neuronal bodies, synapses and dendrites (Vemuri & Jack, 2010; Uylings & de Brabander, 2002), while WMV loss is primarily due to nerve fiber's demyelination (Scheltens et al., 1995). GMV loss is a common feature of AD, according to many studies (Chételat et al., 2007; Frisoni et al., 2002; Karas et al., 2003; 2004) and it correlated positively with

the AD cognitive deterioration (Guo, X. et al., 2010; Guo, Y. et al., 2014). Moreover, sMRI can aid in the early diagnosis of MCI and AD and help monitor the disease progression (Vemuri & Jack, 2010). T1 weighted sequences in sMRI are the best sequence to detect atrophic changes in AD (Johnson, Fox, Sperling & Klunk, 2012)

Structural brain changes in AD include, not only the global brain atrophy/ volume decrease (Double et al., 1996), but also that of some important brain structures such as the hippocampus (Baron et al., 2001; Hua et al., 2008). Brain atrophy is an important AD's structural change (Apostolova et al., 2011) and is correlated with the cognitive deterioration (Fox, Scahill, Crum & Rossor, 1999), with some AD biomarkers such as APOE gene (Agosta et al., 2009) and with some others in the Cerebro Spinal Fluid's (CSF) including tau protein and amyloid plaques (Vemuri et al., 2009). The earliest affected brain structures in AD by the neurofibrillary tangles deposition are the Medial Temporal Lobe (MTL) structures (Arriagada, Growdon, Hedley-Whyte & Hyman, 1992; Braak & Braak 1991; Jack et al., 1999), among which the hippocampus seems to be the earliest affected even before AD clinical manifestations (Fox et al., 1996; Jack, Petersen, O'Brien & Tangalos, 1992; Ridha et al., 2006). Hippocampus volume was found to be the most affected (Chételat et al., 2007; Frisoni et al., 2002), best discriminating CN and AD subjects (Jack et al., 1997) and predictive of MCI to AD conversion (Jack et al., 1999). Hippocampus volume is considered one of the most important existing structural biomarkers of AD, especially in the earliest stages of the disease (Jack et al., 2013; Moon, Lee & Choi, 2018) such as in SMC (Striepens et al., 2010) and MCI (Shi, Liu, Zhou, Yu & Jiang, 2009. Hippocampal atrophy in AD, however, has been found asymmetric (Shi, Liu, Zhou, Yu & Jiang, 2009) and differential along the medial-lateral axis (Zhao et al., 2019) and the anterolateral axis (Greene & Killiany, 2012; Martin, Smith, Collins, Schmitt & Gold, 2010) in different stages of the disease (schuff et al., 2009).

Hippocampus

Hippocampus, an important and complex structure, which can be described as a ''functional polyhedron'' owing to its responsibility for numerous behavioral functions, coordinating them in association with other brain cortical and subcortical structures (Genon, Reid, Langner, Amunts & Eickhoff, 2018). Hippocampus plays a crucial role in memory (Scoville & Milner, 1957; Zola-Morgan, Squire & Amaral, 1986), including some aspects of declarative memory (Cohen & Squire, 1980; Eichenbaum, Otto & Cohen, 1992), more specifically the episodic memory (Bird & Burgess, 2008; Tulving, 2002; Vargha-Khadem, 1997), spatial memory (Abrahams et al., 1999; Burgess, Maguire & O'Keefe, 2002; Maguire, Burgess & O'Keefe, 1999), autobiographic memory (Genon et al., 2018; Viard et al., 2007), relational memory (Eichenbaum & Cohen, 2001; Konkel, 2009) as well as explicit memory (Eichenbaum, 1999; Konkel, 2009). In addition, it is responsible for different learning processes namely encoding (Genon et al., 2018; Grady, McIntosh & Craik, 2003; Horner & Doeller, 2017), consolidation (Nadel & Moscovitch, 1997; Squire, Genzel, Wixted & Morris, 2015) and recollection (Genon et al., 2018; Konkel, 2009). Last but not least, hippocampus appears to be involved in some other higher, more complex cognitive functions including empathy, taking decisions, judgment, creativity and language utilization (Genon et al., 2018; Rubin, Schwarb, Lucas, Dulas & Cohen, 2017). For record, most of these functions are affected in AD, as previously mentioned in the previous section, which highlights the important relationship between Alzheimer's disease and hippocampal atrophy.

Hippocampus organization.

Right and left hippocampi are believed to be asymmetric with regards to structure and function (Maruszak & Thuret, 2014). Regarding the hippocampal volume, for example, there is discrepancy between the left and right hemispheres, where the right hemisphere appears to be larger (Maruszak & Thuret, 2014; Pedraza, Bowers & Gilmore, 2004). With regards to the functional difference, the right side of the hippocampus is believed to be involved more than the left side in the spatial memory, whereas the left hippocampus seem to

be involved more in language processing (Duarte et al., 2014; Hutsler & Galuske, 2003; Shipton et al., 2014).

Hippocampus can be organized into either subfields on the medial-lateral axis or subregions on the anterior-posterior/longitudinal axis (Plachti et al., 2019). Hippocampal subfields' organization into Cornu Ammonis (CA) 1-4, dentate gyrus and subiculum, is based on cytoarchitechtonic histological mapping (Amunts et al., 2005; Zilles, Schleicher, Palomero-Gallagher & Amunts, 2002), which can be done in-vivo and ex-vivo on structural MRI images, using automatic (Van Leemput et al., 2009), semi-automatic (Pluta, Yushkevich, Das & Wolk, 2012) or manual segmentation (Peixoto-Santos et al., 2018) protocols. On the other hand hippocampal organization into subregions, namely head, body and tail, is frequently performed using electrophysiological techniques (Komorowski et al., 2013) or Connectivity Based Parcellation (CBP) (Robinson et al., 2014; Plachti et al., 2019). Hippocampal subregions are believed to be different with regards to the afferent, efferent neuronal networks in rats (Moser and Moser 1998), functional connectivity with other brain regions like the PreFrontal Cortex (PFC) and the Posterior Cingulate Cortex (PCC) (Zarei et al., 2013), gene expression (Fanselov & Dong, 2010), as well as lipid composition and metabolism (Miranda et al., 2019). Moreover it is believed that a functional specialization lies along the longitudinal axis with a possible encoding - retrieval (Prince, 2005), emotion - cognition (Moser & Moser, 1998) and self-centric - world - centric (Plachti et al., 2019) functional gradients.

Voxel Based Morphometry (VBM)

In this project, VBM was used as a preprocessing method for the T1 weighted images to prepare them for further GMV extraction. VBM, which has been introduced first by Ashburner & Friston, 2000, Shah, Ebmeier, Glabus & Goodwin, 1998; Wright et al., 1995; 1999, represents a simple and practical way to detect small-scale differences in the local structure of the brain, including for example brain atrophy, to highlight the neuroanatomical variations in brains of different subjects (Ashburner & Friston, 2000). VBM entails many steps, including Magnetic field inhomogeneity correction, tissue segmentation and spatial normalization. As

a part of or following VBM, statistical tests could be used, in order to detect differences through all voxels in the image, which enables for example detecting volumetric variation across specific brain tissues (Ashburner & Friston, 2000; Whitwell, 2009) in different subjects, such as in the hippocampus' Grey matter (GM). VBM was used by past studies, for instance in highlighting the GM loss in MCI (Baron et al., 2001; Chételat et al., 2002), compare GM loss in early stages of the disease with the normal controls (Hirata et al., 2005), and to investigate hippocampus atrophy milestone along AD progression (Chételat et al., 2008).

Alzheimer's Disease Neuroimaging Initiative (ADNI)

As mentioned previously, our cohort is adapted from The Alzheimer's Disease Neuroimaging Initiative (ADNI). ADNI is a large longitudinal, multicenter study, began in October 2014 as a consortium of various medical centers and universities in the USA (Peterson et al., 2009; Weiner et al., 2013). ADNI has a global goal of detecting, developing and validating various clinical, imaging, genetic and biochemical biomarkers as predictors and outcomes, which might help in the early diagnosis and follow-up of Alzheimer's disease as well as in facilitating subsequent clinical trials with the aim of early Alzheimer's disease detection and treatment (Weiner et al., 2010; 2013). Until now, ADNI has 4 phases including ADNI 1, ADNI GO, ADNI 2, ADNI 3. ADNI enrolled subjects between the ages of 55 and 90, who had a serious of initial clinical, neuropsychological, imaging and genetic testing, some of which were repeated at regular times over the next years after obtaining a written consent. The study had a very big impact in establishing standardized protocols especially in the neuropsychological tests, MRI acquisition and images preprocessing which might facilitate further application in the clinical trials (Weiner et al., 2013). ADNI raw and processed data are available online for the scientific community all over the world. The principle investigator in the study is Michael W. Weiner, M.D., VA medical center and university of San Francisco, California, USA and it was funded by a public-private partnership.

Objectives & Hypothesis

In this project, the hippocampus GMV atrophy along its longitudinal axis in various AD phenotypes compared to normal controls was examined. In addition to that, I tried to approach whether different subregions in the hippocampus were affected in different AD phenotypes. The percentage change of mean hippocampus GMV in each subregion in various disease's phenotypes compared with the normal elderly controls was investigated, which might quantitavely detect the most probable affected subregions in different stages of the disease. As mentioned previously, Hippocampal subregions along its longitudinal axis are supposed to be dissimilar with regards to the afferent, efferent neuronal networks, functional connectivity, behavioral functions, gene expression and lipid composition and metabolism.

In previous studies, it was mentioned that hippocampus GMV was differentially affected along the anterior-posterior axis in different AD stages (Greene & Killiany, 2012; Martin et al., 2010). The Head and Body were mostly affected in MCI (Martin et al., 2010) and in both MCI, AD groups (Greene & Killiany, 2012). Moreover, it was proposed that hippocampus volume is more decreased in later stages of the disease (Greene & Killiany, 2012). Based on that, it is hypothesized that hippocampus GMV would be asymmetrically affected in various AD phenotypes in different subregions along the anterior-posterior axis, where the degree of atrophy would be more pronounced in more advanced AD stages namely AD and LMCI more that the earlier ones such as SMC and EMCI. Moreover the Head and Body subregions should be more affected than the tail.

This study should bring the scientific world a novel insight into investigating the possible effect of early AD stages i.e SMC and EMCI on the hippocampus mean GMV in different subregions. The best stage to medically intervene with AD is the pre-dementia stages (Khan, 2016) to delay the disease progression, which gives a crucial importance to try to find AD markers for these stages and try to validate them. This study could add some evidence for the possible importance of the hippocampus subregions' volumes as an outcome biomarker in possibly detecting a probable AD before dementia occurs. Adapting a hippocampus subregions' model, divided based on the multimodal CBP can aid, in addition, in

complementing the current ongoing research with similar aims, but using different hippocampus models.

Methods

Cohort

The data used in this project was extracted from the ADNI database (http://adni.loni.usc.edu). Subjects were adapted from ADNI phases: ADNI GO, ADNI 2 and ADNI 3. Distribution of subjects between the ADNI phases was as follows: ADNI 2 (771, 79%), ADNI GO (126, 13%) and ADNI 3 (77, 8%). In ADNI, subjects were first selected according to a serious of exclusion-inclusion criteria and then classified into 5 groups according to multiple criteria. All subjects have signed an informed written consent at all sites.

Subject selection.

Subjects recruited by ADNI were subject to a screening visit, in which a serious of neuropsychological, laboratory, clinical and imaging procedures were performed. A serious of inclusion and exclusion criteria was applied (Adapted from ADNI procedures manual: http://adni.loni.usc.edu/methods/documents/).

Inclusion criteria.

1. Age is between 55 and 90 years.
2. Geriatric depression scale (GDS) *(See Box 1)* is below 6.
3. Modified Hachniski score *(See Box 1)* is ≤ 4.
4. Availability of study partner, who has direct contact and/or accompanying the tested subject.
5. Good health condition without known diseases, which might interfere with the study.
6. Visual and auditory capabilities sufficient for neuropsychological testing
7. Fluency in English or Spanish.
8. Completion of 6 grades of education or sufficient work history.

9. Willingness to participate in a longitudinal study.
10. Willingness to undergo repeated MRI scans.

Exclusion criteria.

1- Screening or baseline MRI scans with signs of infection, infarction or focal lesions.
2- Presence of metal objects as Pacemakers and Artificial heart valves.
3- Major depression (Diagnostic and Statistical Manual of Mental Disorders (DSM)-IV criteria) during the previous 1-year as well as any psychotic features in the last 3 months.
4- History of Schizophrenia according to (DSM-IV criteria).
5- Alcohol or substance abuse or dependence in the previous 2 years (DSM IV criteria).
6- Significant medical condition.
7- Significant abnormalities in vitamin B12 or Thyroid Function Tests (TFTs), which might affect the testing protocol.
8- Habitation in skilled nursing facility.
9- Actual use of Warfarin or some psychoactive medications as sedative hypnotics or anxiolytics.
10- Taking part in clinical studies, in which neuropsychological testing occurs, more than once per year.
11- History of cancer five years before screening except for Melanoma.

Subject classification.

Subjects were classified into 5 diagnosis groups based on the following:

- Cognitively Normal (CN) group:
  1- No memory complaints confirmed by the study partner.
  2- Normal memory functions, assessed by Wechsler memory scale – delayed recall scores *(See Box 1),* adjusted to education
     a. ≥ 9 for 16 or more education years
     b. ≥ 5 for 8-15 education years
     c. ≥ 3 for 0-7 education years.

3- Mini-Mental State Exam score (MMSE) between 24 and 30 *(See Box 1).*
4- Clinical Dementia Rating (CDR) score *(See Box 1)* = 0 with the memory component = 0
5- Absence of significant affection of cognitive functions or daily activities.
6- Permitted medication taken in stable doses, for example: Estrogen replacement therapy and antidepressants (lacking significant anticholinergic side effects).

- Subjective Memory Concern (SMC) group: same as CN except for the presence of subjective memory complains, which were reported by the subject, partner or a clinician.

- Early Mild Cognitive Impairment (EMCI) group:
  1- Subjective memory complaints confirmed by subject, the study partner or a clinician.
  2- Abnormal memory functions, assessed by Wechsler memory scale – delayed recall scores adjusted to education
     a. 9-11 for 16 or more education years
     b. 5-9 for 8-15 education years
     c. 3-6 for 0-7 education years.
  3- MMSE score: same as in CN.
  4- CDR score = 0.5 with the memory component at least =0.5
  5- Cognitive functions are preserved and are not diagnosed as Alzheimer's disease by clinician (According to NINCDS/ADRDA criteria).
  6- Permitted medications: same as that in CN in addition to Cholinesterase inhibitors and Memantine, which are permitted until 12 weeks before the screening.
- Late Mild Cognitive Impairment (LMCI) group:
  1- Subjective memory complaints: same as in EMCI.
  2- Abnormal memory functions, assessed by Wechsler memory scale – delayed recall scores adjusted to education.
     a. ≤ 8 for 16 or more education years
     b. ≤ 4 for 8-15 education years

c. ≤ 2 for 0-7 education years.

3- MMSE: same as in CN.
4- CDR and its memory component: same as EMCI.
5- Cognitive functions: same as in EMCI.
6- Permitted medications: same as in EMCI.

- Alzheimer's Disease (AD) group:
  1- Subjective memory complaints: same as in EMCI.
  2- Abnormal memory functions: same as in LMCI.
  3- MMSE score between 20-26
  4- CDR = 0.5 or 1
  5- Cognitive functions: ''Probable AD'' according to NINCDS-ADRDA criteria.
  6- Permitted medications: same as that in EMCI

For each group, additional exclusion parameters were applied as follows:

- CN: significant neurologic disease as Parkinson's disease and Huntington's disease.
- SMC: same as CN.
- EMCI: significant neurologic disease other than possible incipient Alzheimer's disease (another term for MCI).
- LMCI: same as in EMCI.
- AD: significant neurologic disease other than probable Alzheimer's disease.

After subject selection and classification during the screening visit, subjects were scheduled for subsequent visits namely the baseline visit followed by a month 3 visit, month 6 visit and then an annual visit, all in which various neuropsychological and imaging procedures, for follow up and monitoring, were performed.

An important point to take into consideration is that Peterson and colleagues have evaluated the clinical classification of the subjects into 3 groups (CN, MCI, AD) in the ADNI study and found that ADNI has successfully classified these subjects, where the cognitive affection of AD subjects was the highest, even

more than the MCI, whereas no cognitive affection in CN subjects was found (Peterson et al., 2009).

Box 1. Behavioral tests used in subjects' inclusion, exclusion as well as in subjects' classification in ADNI.

Mini Mental State Examination (MMSE): MMSE (Folstein et al., 1975) consists of a serious of tasks, testing different domains with regards to the cognitive functions, including short and long term memory, orientation to time and place, constructional ability and ability to follow commands. The applied MMSE version in ADNI has 10 tasks with maximum score of 30. MMSE is widely used in differentiating subjects with dementia (AD) from the normal control subjects with a moderate sensitivity (79%) and high specificity (95%) (Hancick & Larner, 2011; Khan, 2016), however it shows lower ability in differentiating earlier stages of cognitive affection including the SMC and MCI stages (Benson, Slavin, Tran, Petrella & Doraiswamy, 2005; Mitchell, 2009)

Wechsler memory scale – delayed recall (Wecshler, 1987): is a subtest of the Wechsler memory scale- revised (WMS-R), which is a well known, widely used test battery, serving in memory assessment especially in memory clinics (Clark et al., 2013; Iseki et al., 2010; Kinno et al., 2017). Newer versions of the Wecshler memory scale exist, but the revised version (WMS-R) is still widely used, because it was translated to many other languages (Kinno et al., 2017). Logical memory-delayed recall component represents the verbal memory subset of the WMS-R (Wecshler, 1987; Kawai et al., 2013), which is based on delayed recall (after 30-40 minutes) of a previously presented story components, where the subject is evaluated for each word/unit of the story he recalls, which results in a score, ranging from (0-25) (Wecshler, 1987).

Clinical Dementia Rating scale (CDR) (Morris, 1993): Is a widely used test battery primarily in the AD dementia diagnosis and staging (Morris, 1993; 2001; Williams 2012). It consists of a semi-structured interview with the subject and the informant, designed to detect cognitive decline in 6 categories namely memory, orientation, Judgment and problem solving, community affairs, home and hobbies and personal care (Morris, 1993). It has the advantage of being directly related to proved clinical diagnostic criteria of AD (Morris, McKeel, Fulling, Torack & Berg, 1988). Moreover it shows high degree of stability in dementia severity rating between participants (Williams, Roe & Morris, 2009) and might detect earlier stages of AD dementia as MCI (Morris, 2001) and even pre MCI (Storandt, Grant, Miller & Morris, 2006; Williams, Storandt, Roe & Morris, 2013). It has the disadvantage of being time-consuming. (Khan et al., 2016)

Geriatric Depression Scale (GDS) (Sheikh & Yesavage, 1986): Is a brief questionnaire, composed of 15 questions designed as a screening tool to detect depression in the elderly (Sheikh & Yesavage, 1986). Besides it also shows sensitivity in detecting depression among the elderly, suffering from mild to moderate dementia (Brink, 1984; Sheikh & Yesavage, 1986).

Modified Hachinski score (Rosen, Terry, Fuld, Katzman & Peck, 1980): Is a clinical systematic approach, used to differentiate the AD dementia from the vascular dementia, through completing a form, with relevant neuropsychiatric clinical information about the subject, by a clinician, who is familiar with the patient. This form compromises information about a possible abrupt or gradual cognitive impairment, somatic complains, emotional incontinence, Hypertension history, strokes history, Focal Neurological symptoms (e.g. Seizures and dizziness) and motor Focal Neurological signs (e.g. unequal deep tendon reflexes).

Subjects selected in our study.

Subjects at baseline, to prevent subject repetition, who had T1 weighted, 3 Tesla MRI scans to ensure high image quality, were selected in our study. Total number of subjects was initially 997, who were subject to quality control checks, in which 16 subjects had missing images, 6 subjects had MRI artifacts and 1 subject with missing diagnosis. The final number of subjects was 974.

The 974 subjects were divided according to the diagnosis into 5 groups *(See Table 1, Figure 1)*, where the largest group was the EMCI (N=313, 32%) followed by CN (N = 199, 21%), LMCI (N= 168, 17%), SMC (N= 145, 15%) and then the AD (N= 149, 15%) groups.

Table 1.

Subjects' classification according to the diagnosis.

Diagnosis	Number	Percentage (%)
AD	149	15
CN	199	21
EMCI	313	32
LMCI	168	17
SMC	145	15

Note. Total number was 974 subjects.

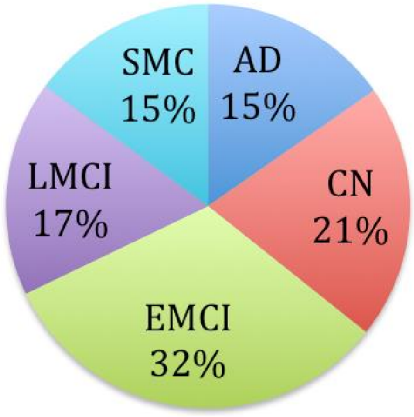

Figure 1. Subjects' classification according to the diagnosis.

Region Of Interest (ROI)

Our ROI was adapted from (Plachti et al., 2019), which is an association from: The Harvard Oxford atlas (Desikan et al., 2006) and the JuBrain cytoarchitectonic atlas (Forschungszentrum Jülich (FZJ), Germany) (Amunts et al., 2005). In the ROI, the total number of voxels was 856 (6920 mm3) in the right hippocampus and 831 (6648 mm3) in the left hippocampus in a 2 mm × 2 mm × 2 mm space (Plachti et al., 2019).

In the current project, the 3-partite hippocampus model, which consists of anterior, intermediate and posterior clusters, along the anterior-posterior axis of the hippocampus, was adapted. Plachti and colleagues used the multimodal CBP to produce these subregions, and their technique is explained in detail in (Plachti et al., 2019). *(See Figure 2).*

Briefly, Connectivity Based Parcellation is a brain mapping technique, which employs functional and anatomical connectivity in defining a brain region/subregion, using each voxel's connectivity profile and thus helps in, not only segregating, but also integrating different brain subregions (Eickhoff et al., 2018; Eickhoff, Thirion, Varoquaux & Bzdok, 2015). This technique can be used, to subdivide the Region Of Interest (ROI) into well-defined subdivisions (Eickhoff, Thirion, Varoquaux & Bzdok, 2015). Due to its reliable regions and subregions definition, CBP can represent an important base for subsequent neuroimaging analysis for studies depending on a CBP defined priori like Voxel Based Morphometry (Eickhoff et al., 2011).

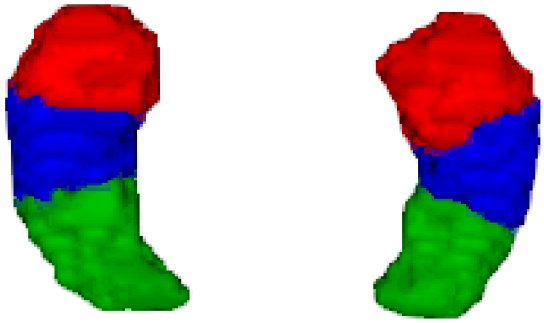

(a) (b)

Figure 2. 3-partite consensus cluster solution based on multimodal functional CBP representing: (a) left hippocampus (b) right hippocampus. The red color represents anterior cluster, blue color represents the intermediate cluster and the green color represents the posterior cluster. Adapted from (Plachti et al., 2019).

MRI Images Acquisition, Preprocessing and Analysis

MRI protocol.

MRI mages were downloaded from the ADNI website (http://adni.loni.usc.edu). Subjects were scanned by standardized MRI protocol, described in (Jack et al., 2008; 2010) (http://adni.loni.usc.edu/methods/mri-tool/mri-analysis/#mri-data-set-container). High-resolution structural MRI scans were acquired from 61 ADNI sites through 3 Tesla scanners. The used scanners were from Siemens medical solutions, Philips medical systems or General Electric health care (GE). Each subject had two (accelerated and non-accelerated) T1 weighted, 3 Tesla MRI scans using a sagittal 3D Magnetization Prepared Rapid Acquisition Gradient Echo (MPRAGE) sequence on Siemens or Philips scanners and a similar pulse sequence, the 3D Inversion Recovery-Fast SPoiled GRass (IR-FSPGR), on GE systems. The following acquisition parameters were applied: Repetition Time (TR) of 2300 ms, Inversion Time (TI) of 853-900 ms, minimum full Echo Time (TE), flip angle of 8-9°, field of view = 256-260 × 240 mm, with 160-170 sagittal 1.2 mm-thick-slices, in a 256 × 256 matrix, yielding a voxel resolution of 1.25 × 1.25 × 1.2 mm, later reconstructed to 1mm isotropic voxels (Hua et al., 2010). With regards to the adapted images for subjects from the ADNI 3, a slightly different protocol described in (Gunter et al., 2017) with the following sequence changes was applied: 208 × 240 × 256 mm field of view, yielding a voxel resolution of 1 × 1 × 1 mm.

MRI images post-acquisition correction for possible artifacts.

In ADNI, a serious of data correction as well as image quality control procedures, performed in Mayo clinic (Rochester, MN, USA) and described in

(Jack et al., 2008). These included revision of each incoming image with regards to image quality, for example the contrast to noise, spatial resolution, resistance to artifacts, protocol compliance and any significant medical aberration. Then images were subject to further series of image pre-processing procedures including 3 steps: image post-acquisition geometric error correction for gradient non-linearity (Jovicich et al., 2006), which corrects geometric distortion of images acquired from multiple sites. Moreover nonparametric intensity non-uniformity normalization is applied to correct for signal intensity non-uniformity, which might result from multiple factors including, for example, the Radiofrequency (RF) coil non-uniformity in MRI scanner (Sled, Zijdenbos & Evans, 1998). This is an important step before tissue segmentation, which requires intensity uniformity for correct classification of each voxel in the correct tissue class (Sled et al., 1998). In addition to that, intensity inhomogeneity correction with regards to receiver coil's sensitivity non-uniformity in the MRI scanner is applied, which, if not corrected, might, not only affect later image processing steps, but also affects image interpretation (Narayana, Brey, Kulkarni & Sievenpiper, 1988). Such steps assure the standardization of the acquired MRI images across different sites, which might give a big chance to capture structural brain differences between subjects, which were not caused by MRI technical non-uniformity or signal inhomogeneities (Jack et al., 2008).

Voxel Based Morphometry (VBM).

In this project, VBM preprocessing was applied using the SPM 12 toolbox (https://www.fil.ion.ucl.ac.uk/spm/software/spm12/; Statistic Parametric Mapping, Institute of Neurology, UCL, London, The UK) as well as the Computational Anatomy Toolbox (CAT) 12.5 (http://www.neuro.uni-jena.de/cat/; structural brain mapping group, Jena university hospitals, Jena, Germany), which is an extension to the SPM 12. The protocol used is in accordance with what has been described in CAT 12.5 manual (http://www.neuro.uni-jena.de/cat12/CAT12-Manual.pdf).

Images were first corrected for inhomogeneities (bias) in the magnetic field and then segmented to Grey Matter (GM), White Matter (WM) and Cerebro-Spinal Fluid (CSF) (Ashburner and Friston, 2005). Segmentation step was done by applying Adaptive Maximum A Posterior (AMAP) technique based on (Rajapakse et al., 1997) to segment the brain into 3 classes: GM, WM and CSF as well as by applying Partial Volume Effects (PVE) (Gaser and Dahnke, 2016; Tohka, Zijdenbos, & Evans, 2004) to further divide the brain into two additional mixed classes namely GM-WM and GM-CSF. By taking these two methods into consideration, each pure tissue fraction in each voxel can be better estimated and thus a better chance exists for more accurate tissue segmentation. Spatial normalization for the image segments followed using the DARTEL algorithm (Ashburner, 2007) and images were normalized to the MNI space. Voxel size of the VBM-preprocessed images was 1 mm × 1 mm × 1 mm. All steps are illustrated more in Box 2.

Spatial Normalization results in what's called deformation field, which illustrates how the local structures are aligned, when matching brains of two subjects together takes place (Kurth et al., 2015). Jacobian matrices are derivatives of the deformation, which encode the local voxel changes (e.g. stretching) within the deformation field. Jacobian determinants are valuable output from these matrices, which indicates how the voxel volume has been changed before and after spatial transformation (Ashburner, 2007). These can be used in order to correct for the volume changes in different segments (e.g. in GM) after spatial Normalization (Kurth et al., 2015).

The modulated, normalized, non linear images were created, by multiplying voxel values with the Jacobian determinant obtained from spatial normalization, which gives an advantage of comparing absolute amount of tissue like GMV in further analysis (Good et al., 2001).

Box 2. Voxel Based Morphometry (VBM) steps employed in this project.

1. **Magnetic field bias correction:** is an essential step before tissue segmentation to act against possible MRI magnetic field inhomogeneity, which might result in different tissue intensities within the same tissue, that are not based on tissue differences, which might affect the automated tissue segmentation step (Ashburner & Friston, 2005; Kurth, Luders & Gaser 2015). Bias might result from static and radio frequency (RF) magnetic fields irregularities, different RF receiver coil sensitivities as well as from different magnetization properties of the object/subject being imaged (Lüdeke, Röschmann & Tischler, 1985; Rajapakse, Giedd & Rapoport, 1997). The effect of bias is more pronounced in high field MRI (T1 weighted) due to the difficulty of keeping homogenous magnetic field intensity with higher field strength (Kurth et al., 2015). Various methods were introduced to act against this possible artifact including various parametric and non-parametric bias correction models, summarized in (Ashburner & Friston, 2005). The used method in our study was based on (Ashburner & Friston, 2005), where the perceived signal was considered as an uncorrupted signal, with added Gaussian noise, covered with bias, where the noise and bias were independent from each others. Noise is based on various properties of different tissues. Bias correction is further bolstered by a set of parameters, which act against smooth intensity variations.

2. **Tissue segmentation**: is based on different tissue intensities, which results in segmenting the brain into WM, GM and CSF with excluding the non-brain components. The segmentation approach used in our study was based on two techniques:

Adaptive Maximum A Posterior (AMAP) segmentation.

AMAP is an automated statistical segmentation technique, which takes into account, not only the biological differences between different tissue types, but also magnetic field intensity inhomogeneity (Rajapakse et al., 1997).

The set of parameters linking the image data to the segmentation process are ion the form of finite Gaussian mixture, which is based on Expectation-Maximization algorithm (EM), which is an iterative method to identify maximum likelihood or Maximum A Posteriori (MAP) estimate of model parameters (Dempster, Laird & Rubin, 1977; Gupta and Chen 2010; Rajapakse et al., 1997). Moreover, the technique depends on the *a priori* 3-D Markov Random Field (MRF) probability model, where the probability of a voxel depends on the neighboring voxels (Rajapakse et al., 1997). This gives the advantage of not only including spatial correlation in the segmentation process, but also to consider signal inhomogenitiy (Held et al., 1997).

Partial Volume Effects (PVE).

A single voxel might contain different tissue types based on the finite resolution of the MRI (Tohka, Zijdenbos & Evans, 2004). This can happen at tissue borders, for instance between brain parenchyma and CSF as well as between GM and WM (Kurth et al., 2015). This means a single voxel is not either GM, WM or CSF but rather more than one tissue type, which means that various signal intensities might be conveyed from different tissues even in the bias corrected images (Kurth et al., 2015). The used technique has Partial Volume (PV) classification step, in which voxels with mixed tissue content are labeled, and Partial Volume Content (PVC) estimation step, where different tissue types in each voxel are estimated (Tohka et al., 2004)

3. **Spatial Normalization:** the Diffeomorphic Anatomical Registeration Through Exponentiated Lie algebra (DARTEL) was applied in this study. DARTEL is a non-linear registration approach, which has the advantage over the linear registration approaches in minimizing the local inter-subject brain (Ashburner, 2007; Stonnington et al., 2007; Kurth et al., 2015). This technique is performed through creating an initial study group/ predefined (in MNI space) DARTEL template, which represents intensity means of the GM and WM (Ashburner, 2007). After each subject's image is registered to this template, a new template is created as the mean of the new images (Ashburner, 2007;Michael, Evans & Moore, 2016). This process is repeated many for a number of times, and after each time the resulting new templates are sharper than the initial one a process called "Coarse-to-fine registration scheme" (Ashburner, 2007). Finally the GM and WM are registered to the final template.

ROI analysis.

Mean GMV was extracted from the before-mentioned ROI, for each participant in the following steps. The first step was creating masks for the ROI, which were then 3D resampled using the AFNI package (Cox, 1996; afni.nimh.nih.gov) to the MNI space containing the preprocessed T1 weighted images, with the same resolution. This is to make sure that the resampled ROIs fit the dimensions, space, and orientation and have the same voxel size as our preprocessed T1 weighted images, before extracting any data from them. In the next step, average GMV was then extracted for each participant from the ROI, using the fslstats function in the FSL package (Jenkinson, Beckmann, Behrens, Woolrich & Smith, 2012; Smith et al., 2004; Woolrich et al., 2009) (https://fsl.fmrib.ox.ac.uk/fsl/fslwiki/FSL).

Statistical Analysis

A two-way ANalysis of COVAriance (ANCOVA) was performed to investigate whether the hippocampus mean GMV is differential in different subregions, in different diagnosis phenotypes of AD. Statistical analysis was performed using the JASP software (https://jasp-stats.org). Significance levels were set at P< .05.

Results

Descriptive Statistics: In this section I will focus on the age, education and gender distribution in the cohort and I will describe some of the behavioral tests' results for the cohort.

Demographic characteristics – Age and Education.

The mean Age *(See Table 2, Figure 3)* in all diagnosis groups was arranged as follows: in an ascending order, the lowest mean was the EMCI group (M=71, SD=7.52) then LMCI (M= 72.2, SD= 7.57), SMC (M= 72.2, SD= 5.79), CN (M=73, SD=6.4) and AD (M = 74.5, SD= 8.3) groups. Means in the 5 groups were not significantly different from each other at P Bonferroni of < .001, except between (AD, SMC) groups and (EMCI, SMC) groups.

The mean Education *(See Table 2, Figure 4)* was arranged as follows: in an ascending order, the lowest mean was in the AD group (M =15.80, SD= 2.605) followed by EMCI (M= 15.89, SD= 2.643), LMCI (M= 16.42, SD= 2.584), CN (M= 16.48, SD= 6.452), and then SMC (M= 16.88, SD= 2.475) groups. Means are not significantly different from each other except between (AD, EMCI), (AD, LMCI) and (CN, EMCI) groups, at P Bonferroni of < .001.

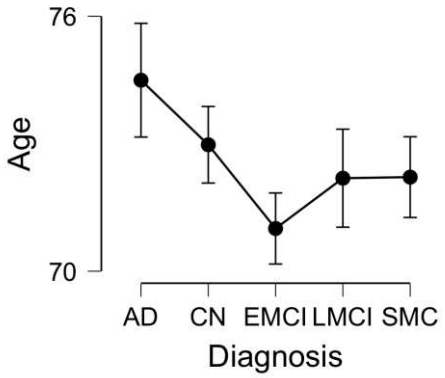

Figure 3. Age plot versus Diagnosis.

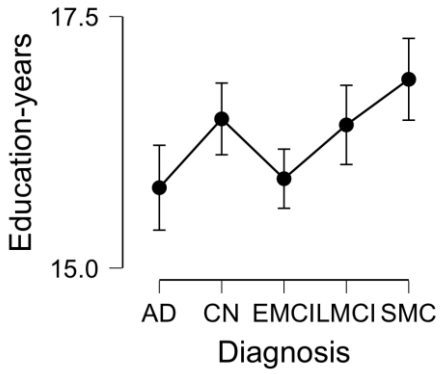

Figure 4. Education plot versus Diagnosis.

Table 2.

Demographic characteristics – age and education.

	Diagnosis	Mean	SD	Minimum	Maximum	N
Age	CN	72.98	6.452	55.80	89.00	199
	SMC	72.21	5.786	58.70	90.30	145
	EMCI	71.00	7.519	55.00	88.60	313
	LMCI	72.19	7.570	55.00	91.40	168
	AD	74.49	8.268	55.90	90.30	149
Education	CN	16.48	2.548	12.00	20.00	199
	SMC	16.88	2.475	8.000	20.00	145
	EMCI	15.89	2.643	10.00	20.00	313
	LMCI	16.42	2.584	9.000	20.00	168
	AD	15.80	2.605	9.000	20.00	149

Note. Measurements were in years. SD is the Standard Deviation. N is the Number of subjects.

Demographic characteristics – Gender.

With regards to the Gender *(See Table 3),* the male-female numbers and percentages were different among different groups. The male number and percentage were higher in the AD group (85, 57%), EMCI (171, 55%) and in the

LMCI (89, 53%) groups. On the other hand the female number and percentage were higher in the CN (110, 55%) and SMC (87, 60%).

Table 3.

Demographic characteristics – Gender.

		Male		Female		
		Number	**Percentage**	**Number**	**Percentage**	**Total number**
Gender	CN	89	45%	110	55%	145
	SMC	58	40%	87	60%	149
	EMCI	171	55%	142	45%	313
	LMCI	89	53%	79	47%	168
	AD	85	57%	64	43%	199

Behavioral characteristics.

Regarding the Mini Mental State Examination (MMSE) test scores *(See Table 4, Figure 9),* the highest mean was the SMC group (M= 29.12, SD= 1.121) followed by CN (M= 29, SD=1.24), EMCI (M= 28.3, SD=1.56), LMCI (M=27.6, SD=1.82) and AD (M=23.1, SD=2.08).

With regards to the Wechsler memory scale – delayed recall test results *(See Table 4, Figure 10),* the highest mean was in the CN group (M= 13.4, SD= 3.05) followed by SMC (M= 13.2, SD=3.21), EMCI (M= 8.88, SD=1.77), LMCI (M= 3.99, SD= 2.67) and AD (M= 1.47, SD= 1.87).

With regards to the Clinical Dementia Rating (CDR) results *(See Table 4, Figure 11),* the highest mean was in the AD group (M= 4.48, SD= 1.71) followed by LMCI (M= 1.76, SD=0.1), EMCI (M= 1.28, SD=0.75), SMC (M= 0.05, SD= 0.15) and CN (M= 0.03, SD= 0.13).

For the 3 tests, all means in the 5 groups are significantly different from each other except between the (CN, SMC) groups, at P Bonferroni of $< .001$.

Table 4.

Behavioral scores in each diagnosis group.

	Diagnosis	Mean	SD	Minimum	Maximum	Valid	Missing
Mini Mental	CN	29.03	1.241	24.00	30.00	199	0
State	SMC	29.12	1.121	24.00	30.00	145	0
Examination	EMCI	28.31	1.564	23.00	30.00	313	0
(MMSE)	LMCI	27.62	1.817	24.00	30.00	168	0
score	AD	23.07	2.075	19.00	26.00	149	0
Wecshler	CN	13.43	3.054	7.000	21.00	199	0
memory	SMC	13.21	3.208	5.000	23.00	145	0
scale	EMCI	8.881	1.774	5.000	15.00	312	1
delayed	LMCI	3.994	2.672	0.000	11.00	167	1
recall score	AD	1.470	1.866	0.000	8.000	149	0
Clinical	CN	0.03266	0.1337	0.000	1.00	199	0
Dementia	SMC	0.05172	0.1528	0.000	0.5000	145	0
Rating	EMCI	1.276	0.7529	0.5000	4.00	313	0
(CDR) score	LMCI	1.762	0.9999	0.5000	5.500	168	0
	AD	4.483	1.707	1.000	10.000	149	0

Note. SD is the Standard Deviation.

Effect of Alzheimer's Disease Stage on The Hippocampus Mean GMV on Both Hemispheres

Two- way ANCOVA- left hemisphere.

A two-way ANCOVA was performed on the left hippocampus to investigate, if there is differential affection of the left hippocampus subregions' mean GMV in different AD diagnosis groups. The model has 2 factors, in which the first factor was the cluster (3 clusters, including the anterior, intermediate and posterior

clusters), and the second factor was the diagnosis (5 diagnosis groups, including AD, CN, EMCI, LMCI and SMC). The dependent variable was the left hippocampus clusters' mean GMV. Covariates were age, gender and education. Through ANCOVA we could investigate the main effects of the Cluster and Diagnosis on the left hippocampus GMV as well as the interaction effects between the 2 factors with regards to the mean GMV, all of which after controlling for age, education and gender. This is to see the possible differential affection of left hippocampus GMV in different subregions in various diagnosis groups and see the potential dependency of the left hippocampus atrophy on the AD stage.

Main & interaction Effects.

Results *(See Table 6)* suggested that there were significant main effects of the diagnosis ($F(4,2904) = 230$, $p < .001$, $\eta_p^2 = 0.158$) and the cluster ($F(2, 2904) = 631$, $p < .001$, $\eta_p^2 = 0.217$) on the left hippocampus mean GMV. In addition to that, there was no significant interaction effect between cluster and diagnosis ($F(8, 2904) = 0.8$, $p = .601$, $\eta_p^2 = 0.001$), with this regard *(See Table 6)*.

Table 6.

Two-way ANCOVA results

	Sum of Squares	**df**	**Mean Square**	**F**	**p**	**η^2**
Cluster	6.567	2.000	3.284	630.633	< .001	0.217
Diagnosis	4.782	4.000	1.195	229.577	< .001	0.158
Cluster * Diagnosis	0.033	8.000	0.004	0.802	0.601	0.001
Age	2.798	1.000	2.798	537.291	< .001	0.092
Gender	0.946	1.000	0.946	181.637	< .001	0.031

Education-years	0.006	1.000	0.006	1.136	0.287	0.000
Residual	15.121	2904.000	0.005			

Note. Type III Sum of Squares. The df is the degree of freedom, F is the F ratio adjusted to the covariates and the η^2 represents the effect size.

In the left anterior cluster, the AD group (M = 0.527, SD = 0.088) had the smallest mean GMV followed by the LMCI (Mean = 0.592, SD = 0.099), the EMCI (M = 0.626, SD = 0.090), the SMC (M = 0.663, SD = 0.063) and then the CN (M = 0.657, SD = 0.067) groups.

With regards to the left intermediate cluster, similar results to the anterior cluster were present, with the AD group (M = 0.469, SD = 0.088) having the smallest mean GMV, followed by the LMCI (M = 0.528, SD = 0.099), the EMCI (M = 0.569, SD = 0.087), the SMC (M = 0.596, SD = 0.065) and then the CN (M = 0.605, SD = 0.067) groups.

Regarding the left posterior cluster, there were also similar results to the previously mentioned clusters, where the mean GMV was the lowest in the AD group (M = 0.411, SD = 0.080) followed by the LMCI (M = 0.459, SD = 0.091), EMCI (M = 0.514, SD = 0.084), SMC (M = 0.537, SD = 0.062) and CN (M = 0.540, SD = 0.065) groups.

All of the results are summarized in table 7 and represented on figure 5.

Table 7.

Descriptives - the Clusters' mean GMVs with the Standard Deviation (SD) *on the left Hemisphere*.

Cluster	**Diagnosis**	**Mean**	**SD**	**N**
Left anterior cluster	CN	0.657	0.067	199
	SMC	0.663	0.063	145
	EMCI	0.626	0.090	313

	LMCI	0.592	0.099	168
	AD	0.527	0.088	149
Left intermediate cluster	CN	0.605	0.067	199
	SMC	0.596	0.065	145
	EMCI	0.569	0.087	313
	LMCI	0.528	0.100	168
	AD	0.469	0.088	149
Left posterior cluster	CN	0.540	0.071	199
	SMC	0.537	0.062	145
	EMCI	0.514	0.084	313
	LMCI	0.459	0.091	168
	AD	0.411	0.080	149

Note. Volume measurements are in mm^3 and they represent the mean GMV. SD is the Standard Deviation and N is the number of subjects.

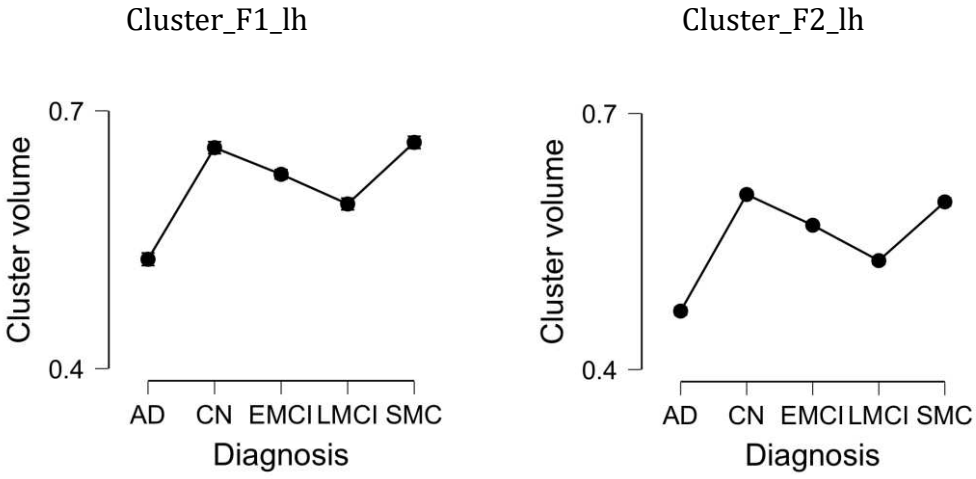

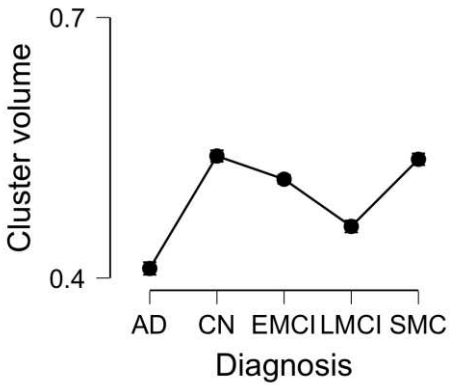

Figure 5. Clusters' mean GMV in each diagnosis group on the left hemisphere.

Post Hoc Comparisons – Cluster.

Since the Cluster has significant main effect, Post Hoc Comparisons Bonferroni correction *(See Table 8)* were done to examine which clusters specifically differ from the other with respect to GMV. Results have shown that there were significant differences between the left anterior cluster, left intermediate cluster and left posterior cluster regarding their GMV, where ($p_{bonf} < .001$).

Table 8.

Post Hoc Comparisons – Cluster.

		Mean Difference	**SE**	**t**	**p bonf**
Left anterior cluster	Left intermediate cluster	0.060	0.003	17.564	< .001
	Left posterior cluster	0.121	0.003	35.514	< .001
Left intermediate cluster	Left posterior cluster	0.061	0.003	17.950	< .001

Post Hoc Comparisons – Diagnosis.

Because the Diagnosis had a significant main effect, Post Hoc Comparisons were performed, using t Test with Bonferroni correction *(See Table 9),* to examine which diagnosis group differs from the other with respect to the GMV. Results suggested that there were significant differences between all diagnosis groups (AD, CN, EMCI, LMCI and SMC) with regards to the left hippocampus mean GMV, (p_{bonf} < .001) except for the CN and SMC, which were not significantly different from each other (p_{bonf} = 1).

Table 9.

Post Hoc Comparisons – Diagnosis.

		Mean Difference	**SE**	**t**	**p bonf**
CN	SMC	0.003	0.008	0.370	1.000
	EMCI	0.037	0.006	5.929	< .001
	LMCI	0.073	0.007	10.255	< .001
	AD	-0.120	0.008	-15.741	< .001
SMC	EMCI	-0.035	0.007	-4.836	< .001
	LMCI	-0.070	0.008	-8.916	< .001
	AD	-0.117	0.008	-14.067	< .001
EMCI	LMCI	0.036	0.007	5.477	< .001
	AD	-0.083	0.007	-11.713	< .001
LMCI	AD	-0.047	0.008	-6.030	< .001

To summarize, there is significant differential left hippocampus atrophy in the 3 subregions between different AD diagnosis groups except between the CN and SMC groups. In addition to that, the hippocampus atrophy appears to be more pronounced in all 3 clusters, in the groups with advanced disease stage like AD groups more than LMCI, EMCI and SMC groups, all of which are arranged in

ascending order with respect to mean GMV. Last but not least, left hippocampus atrophy was dependent on which diagnosis group the subject is in.

Two- way ANCOVA- right hemisphere.

A two-way ANCOVA was performed to investigate, if there is differential affection of the right hippocampus' mean GMV along the three subregions in different AD diagnosis phenotypes. The first factor was the diagnosis (5 diagnosis groups, including AD, CN, EMCI, LMCI and SMC), and the second factor was the clusters (3 clusters including the anterior, intermediate and posterior clusters. The dependent variable was the right hippocampus clusters' mean GMV. The covariates were age, gender and education. This was to examine the probable differential affection of the right hippocampus GMV in various subregions in all the 5 diagnosis phenotypes and whether hippocampus atrophy is dependent on the diagnosis group.

Main & interaction Effects.

Results *(See Table 12, 13)* have shown that there was a significant main effect of the cluster on the right hippocampus mean GMV ($F (2, 2904) = 816$, $p < .001$, $\eta_p^2 = 0.273$). In addition to that, there was a significant main effect of the diagnosis ($F (4, 2904) = 196$, $p < .001$, $\eta_p^2 = 0.131$) *(See Table 14).* Moreover, there was a significant interaction effect between cluster and diagnosis ($F (8, 2904) = 2.18$, $p = .026$, $\eta_p^2 = 0.003$) *(See Table 10).* All results are after controlling for age, gender and education.

Table 10.

Two-way ANCOVA results

	Sum of Squares	**df**	**Mean Square**	**F**	**p**	**η^2**
Cluster	9.042	2.000	4.521	816.206	< .001	0.273

Diagnosis	4.342	4.000	1.085	195.955	< .001	0.131
Cluster * Diagnosis	0.097	8.000	0.012	2.179	0.026	0.003
Age	2.868	1.000	2.868	517.802	< .001	0.087
Gender	0.709	1.000	0.709	127.962	< .001	0.021
Education-years	0.005	1.000	0.005	0.944	0.331	0.000
Residual	16.085	2904.000	0.006			

Note. Type III Sum of Squares. The df is the degree of freedom, F is the F ratio adjusted to the covariates and the η^2 represents the effect size.

The mean GMV was estimated in various clusters in different diagnosis groups. In the right anterior cluster, the AD group (M = 0.412, SD = 0.073) had the smallest mean GMV followed by the LMCI (Mean = 0.452, SD = 0.080), the EMCI (M = 0.498, SD = 0.076), the SMC (M = 0.513, SD = 0.061) and then the CN (M = 0.518, SD = 0.069) groups.

With regards to the right intermediate cluster, similar results to the anterior cluster were present with the AD group (M = 0.464, SD = 0.102) having the smallest mean GMV followed by the LMCI (M = 0.528, SD = 0.112), the EMCI (M = 0.579, SD = 0.096), the SMC (M = 0.604, SD = 0.061) and then the CN (M = 0.612, SD = 0.078) groups.

For the right posterior cluster, there were similar results to the other two clusters, where the mean GMV was the lowest in the AD group (M = 0.541, SD = 0.089) followed by the LMCI (M = 0.598, SD = 0.096), EMCI (M = 0.636, SD = 0.086), SMC (M = 0.660, SD = 0.065) and CN (M = 0.665, SD = 0.067) groups.

All of the results are summarized in table 11 and figure 6.

Table 11.

Descriptives - the Clusters' mean GMVs with the SD *on the right Hemisphere.*

Cluster	Diagnosis	Mean	SD	N
Right anterior cluster	CN	0.518	0.069	199
	SMC	0.513	0.061	145
	EMCI	0.498	0.076	313
	LMCI	0.452	0.080	168
	AD	0.412	0.073	149
Right intermediate cluster	CN	0.612	0.078	199
	SMC	0.604	0.076	145
	EMCI	0.579	0.096	313
	LMCI	0.528	0.112	168
	AD	0.464	0.102	149
Right posterior cluster	CN	0.665	0.067	199
	SMC	0.660	0.065	145
	EMCI	0.636	0.086	313
	LMCI	0.598	0.096	168
	AD	0.541	0.089	149

Note. Volume measurements are in mm^3 and they represent the mean GMV. SD is the Standard Deviation. N is the Number of subjects.

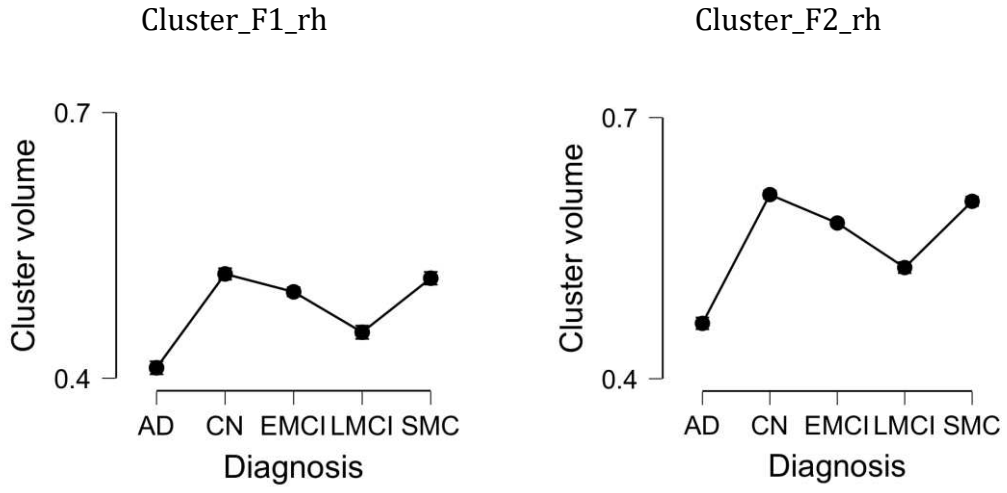

Cluster_F3_rh

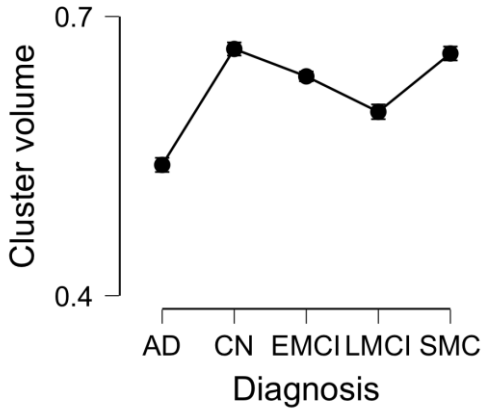

Figure 6. Descriptives plots for the clusters' mean GMVs, in each diagnosis group, on the right hemisphere.

Post Hoc Comparisons – Cluster.

Clusters on the right hemisphere had significant main effect as well, consequently Post Hoc Comparisons were performed using Bonferroni correction *(See Table 12)* and there were significant differences between the right anterior cluster, right intermediate cluster and right posterior cluster with regards to the mean GMV, where $p_{bonf} < .001$.

Table 12.

Post Hoc Comparisons – Cluster.

		Mean Difference	**SE**	**t**	**p bonf**
Right anterior cluster	Right intermediate cluster	-0.079	0.004	-22.436	< .001
	Right posterior cluster	-0.141	0.004	-40.317	< .001
Right	Right posterior	-0.063	0.004	-17.882	< .001

intermediate cluster	cluster				

Post Hoc Comparisons – Diagnosis.

Diagnosis had a significant effect on the mean GMV, so Post Hoc Comparisons using t Test with Bonferroni correction were done *(See Table 13).* Results have shown that there were significant differences between all diagnosis groups (AD, CN, EMCI, LMCI and SMC) with regards to the right hippocampus mean GMV, where ($p_{bonf} < .001$), except for the CN and SMC, which were not significantly different from each other with this regard, where ($p_{bonf} = 1$).

Table 13.

Post Hoc Comparisons – Diagnosis.

		Mean Difference	**SE**	**t**	**p bonf**
CN	SMC	0.007	0.008	0.881	1.000
	EMCI	0.034	0.006	5.218	< .001
	LMCI	0.072	0.007	9.874	< .001
	AD	-0.114	0.008	-14.673	< .001
SMC	EMCI	-0.027	0.007	-3.657	0.003
	LMCI	-0.065	0.008	-8.071	< .001
	AD	-0.107	0.009	-12.616	< .001
EMCI	LMCI	0.038	0.007	5.749	< .001
	AD	-0.081	0.007	-11.193	< .001
LMCI	AD	-0.042	0.008	-5.332	< .001

Post Hoc Comparisons – Interaction between Cluster and Diagnosis.

Since there is significant interaction between the cluster and diagnosis, post-hoc analysis for this interaction was done, to see more specifically which cluster

interacts with which diagnosis group with respect to GMV. Results suggest that there is significant interactions between all diagnosis groups and all clusters at $p_{bonf} < .001$ *(See Table 14).*

Table 14.

*Marginal means- Cluster * Diagnosis*

				95% CI			
Cluster	**Diagnosis**	**Marginal Mean**	**SE**	**Lower**	**Upper**	**t**	**p**
Right anterior cluster	CN	0.519	0.005	0.503	0.534	98.158	< .001
	SMC	0.509	0.006	0.490	0.527	82.028	< .001
	EMCI	0.493	0.004	0.481	0.506	116.773	< .001
	LMCI	0.452	0.006	0.435	0.469	78.703	< .001
	AD	0.424	0.006	0.406	0.442	69.267	< .001
Right intermediate cluster	CN	0.612	0.005	0.597	0.628	115.903	< .001
	SMC	0.600	0.006	0.581	0.618	96.682	< .001
	EMCI	0.575	0.004	0.562	0.587	136.035	< .001
	LMCI	0.528	0.006	0.511	0.545	91.901	< .001
	AD	0.476	0.006	0.458	0.493	77.734	< .001
Right posterior cluster	CN	0.666	0.006	0.650	0.681	126.049	< .001
	SMC	0.656	0.004	0.638	0.674	105.786	< .001
	EMCI	0.631	0.006	0.619	0.644	149.483	< .001
	LMCI	0.598	0.006	0.581	0.615	104.071	< .001
	AD	0.552	0.006	0.534	0.570	90.312	< .001

Note. Bonferroni CI adjustment. CI is the Confidence Interval.

To sum up, there is significant differential right hippocampus atrophy in the 3 subregions between various AD diagnosis groups except between the CN and SMC groups. Moreover, the right hippocampus atrophy seems to be more prominent in all 3 clusters, in the groups with later disease stage as AD group more than LMCI,

EMCI and SMC groups. Finally the right hippocampus atrophy in each cluster is dependant on the AD stage.

Which subregions might be more affected more than the others in different disease stages?

In this section, the percentage differences between different diagnosis groups (EMCI, LMCI and AD) and the CN group with regards to the hippocampus mean GMV in different clusters on the right and left hemispheres were investigated. This is measured by subtracting each group's mean GMV value from the CN group's and then dividing the resulting difference by the CN groups GMV value, followed by multiplying the result by 100 to get the percentage. This can give an additional insight, through 'quantitatively' highlighting the most affected clusters in different disease-related diagnosis groups.

As mentioned previously the diagnosis groups were significantly different from each other in terms of mean hippocampal GMV on each of the left and right hemispheres except for the CN and SMC groups. Consequently the results on this section were focused only on the EMCI, LMCI and AD group's differences from the CN.

As shown in Tables 15a and 15b, the most probable affected clusters in the EMCI were the left and right intermediate clusters, where the left Intermediate cluster had -5,95% and the right intermediate cluster had -5,39% percentage differences. On the other hand, the most affected clusters in LMCI were the right intermediate cluster with -13,7% and the left posterior cluster with -15% percentage differences. In the AD group, the most probable affected clusters were the same as in LMCI but with higher percentage difference, in which the right intermediate cluster had -24,9% and the left posterior clusters had -23,9% percentage differences.

Table 15a.

Clusters mean GMV and percentage difference of each diagnosis group (AD and EMCI) from Cognitively Normal (CN) diagnosis group.

Cluster	CN	SMC		EMCI	
	GMV	GMV	% Difference	GMV	% Difference
Left anterior cluster	0,657	0,663	0,9132	0,626	-4,72
Left Intermediate cluster	0,605	0,513	-0,96	0,569	**-5,95**
Left posterior cluster	0,54	0,596	**-1,48**	0,514	-4,81
Right anterior cluster	0,518	0,604	**-1,3**	0,498	-3,86
Right intermediate cluster	0,612	0,537	-0,55	0,579	**-5,39**
Right posterior cluster	0,665	0,66	-0,75	0,636	-4,36

Note. Volume measurements are in mm^3 and they represent the mean GMV.

Table 15b.

Clusters mean GMV and percentage difference of each diagnosis group (LMCI and SMC) from Cognitively Normal (CN) diagnosis group.

Cluster	LMCI		AD	
	GMV	% Difference	GMV	% Difference
Left anterior cluster	0,592	-10	0,527	-19,8
Left intermediate cluster	0,452	-12	0,469	-22,48
Left posterior cluster	0,528	-12,73	0,411	**-23,89**
Right anterior cluster	0,528	**-13,73**	0,412	-20,46
Right intermediate cluster	0,459	**-15**	0,464	**-24,18**
right posterior cluster	0,598	-10,1	0,541	-18,65

Note. Volume measurements are in mm^3 and they represent the mean GMV.

Discussion

The aim of the study was to explore the possible differential affection of different hippocampus subregions in various AD diagnosis phenotypes in ADNI. We used subjects data from ADNI with 3T, T1-weighted structural MRI images, preprocessed them with VBM prior to GMV extraction using FSL package. Results suggested that there was asymmetric hippocampus affection along its longitudinal axis in different diagnosis groups. Moreover, the hippocampus shrinkage was more in later disease stages more than the earlier in all subregions. Besides, The right hippocampus atrophy appeared to be dependent on the disease stage. Finally the most affected clusters were the right, left intermediate and the left posterior subregions in different studied AD phenotypes. In the following, I will try to interpret the results and highlight some of the used techniques in relation to some of the past and current literature.

Differential Affection of Hippocampus Subregions along AD Progression

From the results, it was evident that there was differential affection of the mean GMV in different clusters along the anterior-posterior axis of the hippocampus in various AD diagnosis phenotypes. These results were in accordance with, what was described by some authors about the longitudinal gradient of not only the volume change, but also of that of the pathology, behavioral changes, metabolic changes, functional correlations and genetic representation in different hippocampus subregions, taking place in AD.

With regards to the hippocampus volume change, it was evident across multiple studies that there was differential volume change along the longitudinal axis of the

hippocampus during different stages of AD, yet the pattern of this change proved to be inconsistent across them. Hippocampal subregional volumes were significantly different between AD, MCI and normal controls, where AD subjects were most affected, followed by MCI subjects (Greene & Killiany, 2012; Martin et al, 2010; Maruszak & Thuret, 2014). Moreover, hippocampus atrophy in AD was found to be more pronounced in the anterior part i.e. the head, in AD subjects (Raji et al., 2009) and in MCI subjects (Martin et al., 2010) compared to healthy controls. It was proposed in addition that the anterior hippocampus could best predict the conversion to AD (Apostolova et al., 2006; Costafreda et al., 2011). However, in some other studies symmetric hippocampus atrophy was evident along the anterior-posterior axis in AD subjects (Chan et al., 2001; Laakso et al, 2000) and in MCI subjects (Echávarri et al., 2011). In another study, the most significant change was found to be in the head and body in both the MCI and AD groups with no significant difference between both groups, indicating the early involvement of these subregions along AD progression (Greene & Killiany, 2012).

In our study, significant differences between the different diagnosis groups i.e. EMCI, LMCI, AD were found, compared with normal controls, where the AD subjects were most affected followed by LMCI and EMCI subjects. However the most affected clusters were the left and right intermediate clusters i.e. the body in EMCI, and the right intermediate and left posterior clusters in both the LMCI and AD, which is quite different from the anterior hippocampus atrophy pattern, found in some other previous studies. Discrepancy of our study from other studies as well as in between these studies themselves might be attributed to the differences in the adapted ROI model, which entails different techniques to cluster/segment the hippocampus.

Other hippocampus pathologic changes in AD appeared to have an anterior-posterior gradient. The anterior hippocampus was found to be the earliest affected hippocampus part with neurofibrillary tangles (Braak & Braak, 1995). Tau Proteins deposition is differential along the hippocampus' longitudinal axis and was found to be corresponding to the most atrophied subregions in AD subjects (Frankó & Joly, 2013). Besides, the hippocampus body was found to be more correlated to the CSF amyloid accumulation in MCI subjects (Carmichael, Xie,

Fletcher, Singh & DeCarli, 2012). Dementia's severity in AD subjects, measured by CDR score, was more in the hippocampus' head than the body and tail (Gordon, Blazey, Benzinger & Head, 2013). Furthermore, glucose metabolism was significantly lower in hippocampus head in AD subjects (Ouchi et al., 1998). Moreover, functional correlation of the hippocampus' subregions with other brain regions was found different, when comparing AD subjects with healthy controls, which might be related to the behavioral affection pattern, observed in AD (Zarei et al. 2013). While the functional correlation of the hippocampus head with PFC was stronger in AD subjects than healthy controls, the correlation of the hippocampus body with the PCC was weaker in AD subjects than in healthy controls (Zarei et al. 2013). Finally, the differential gene expression along the longitudinal axis could aid in explaining the dissimilar variability of hippocampus subregions' affection in AD, where the posterior subregion seemed to be more vulnerable than the anterior subregion to AD as described in (Vogel et al. 2019). All these changes might contribute to the before-mentioned subregional volumetric variations found in our study as well as in some other studies.

Importance of Hippocampus Subregion's Atrophy Detection Using Structural MRI in Comparison to Other Alzheimer's Disease Markers in Tracing AD

Different AD biomarkers are considered so important in AD detection, that they were incorporated in the diagnostic criteria, which have been introduced by the NIA-AA and the IWG as supportive tools for probable AD diagnosis. Biomarkers reflect the biological events occurring in the AD along its progression (Dubois et al., 2014). Biomarkers represent supportive diagnostic tools for suspecting and tracking of early asymptomatic and symptomatic AD (Dubois et al., 2014).

Probable AD diagnosis includes a core clinical criterion, supportive criteria, and exclusion criteria (Dubois et al., 2007). As mentioned previously, some imaging markers such as hippocampus atrophy were included among the supportive criteria as they are important tools for tracing certain pathological alterations

taking place in AD, and they correlated with the AD behavioral changes. Other markers include volume loss of other MTL structures such as entorhinal cortex, CSF biomarkers namely the beta amyloid and tau proteins, PET imaging markers such as glucose metabolism change, as well as genetic alteration. MRI markers namely MTL atrophy was found to be more effective in differentiating MCI and AD subjects from normal controls than the CSF biomarkers, in another words, it reflects the underlying clinical stage better (Vemuri et al., 2009). However combination between structural imaging and CSF biomarkers has been found more effective than each group alone in predicting the diagnosis group i.e. CN, MCI and AD (Vemuri et al., 2009). Another study revealed that combining MRI, CSF and neuropsychological measures was able to discriminate the 3 diagnosis groups and predict, who from the MCI will/will not convert to AD (Greene & Killiany, 2012). On the other hand, CSF and PET imaging biomarkers are believed to be detectable prior to the MRI biomarkers in the course of AD progression because they reflect the etiology of the disease, and they might be able in addition to be detected in subjects at risk of developing AD i.e preclinical/asymptomatic AD (Dubois et al., 2014). Diagnostic precision depends on the choice of the marker and the protocol used for each (Frisoni et al., 2013). This raises the importance of developing standardized protocols for acquisition and analysis of all the markers, an effort done by ADNI, which will enhance the biomarker's benefit in being powerful diagnostic tools in early AD detection (Frisoni, Fox, Jack, Scheltens & Thompson, 2010; Weiner et al., 2013).

Hippocampus atrophy rate reflects the neurodegeneration occurring in AD, and is used as an outcome measure for clinical trails involving disease-modifying therapies (Frisoni, Fox, Jack, Scheltens & Thompson, 2010). Whole hippocampus atrophy was not found as sensitive as atrophy of particular hippocampus subfields/subregions as a marker for AD (Apostolova et al., 2006; Maruszak & Thuret, 2014). Some authors claim that atrophy of some other MTL structures such as Entorhinal cortex might be more sensitive than hippocampus atrophy in detecting insipient AD i.e. MCI (Dickerson et al., 2001), as well as in reflecting underlying pathology (Dubois et al., 2007), However measuring its volume change is technically more difficult than the hippocampus (Du et al, 2001). A combination

of different MTL structures atrophy might be a more sensitive way in capturing early AD (Dubois et al., 2007). An important challenge to consider, with regards to the MTL structures atrophy, is that it might happen as well in other types of non-AD dementia disorders such as vascular dementia and hippocampus sclerosis, in other neurodegenerative conditions such as argyrophilic grain disease (Dubois et al., 2007; Jicha et al, 2006), as well as in Depression, in which hippocampus atrophy might happen (Bremner et al., 2000). However, careful clinical and psychological screening, employing other supportive criteria as the previously mentioned CSF biomarkers, and with the presence of exclusion criteria for such conditions might help differentiating atrophy on top of AD and non-AD dementias. This stresses the importance of combination of different measures beside the hippocampus atrophy in the diagnosis of probable AD, and gives an additional motive to study in depth the differential hippocampus subregion/subfield in different types of AD and non-AD dementias.

Voxel Based Morphometry, A Reliable Method to Detect Hippocampus Volume Changes?

Voxel Based Morphometry (VBM) is a dependable technique, used to detect voxel-wise structural brain volumetric changes on T1 weighted sMRI images, which not only reflects the underlying biological brain changes such as GM/WM loss (Ashburner & Friston, 2001), but also enables further comparisons of the volume changes across all image's voxels between different subjects, using statistical methods. VBM showed to be a sensitive and an objective method in detecting regional small-scale structural brain differences across different individuals (Mechelli, Price, Friston & Ashburner, 2005). VBM has helped many researchers to investigate the effect of Alzheimer's disease (Chételat et al., 2005), Schizophrenia (Meisenzahl et al., 2008), bipolar disorder (Brown et al., 2012), aging (Good et al., 2001), gender (Smith et al., 2007), genetic composition (Campbell et al., 2006), and developmental disorders (Silani et al., 2005) on the structure of the brain. In Alzheimer's disease, VBM showed to be sensitive in detecting GM changes,

occurring early in the disease (Chételat et al., 2002; Pennanen, 2005), including the hippocampus changes (Chételat et al., 2008).

On the other hand, interpretation of VBM-processed data across multiple studies might be challenging, owing to the difference of sample sizes, preprocessing steps and MRI protocols, which might affect the results (Whitwell, 2009). In addition to that, the efficiency of the spatial normalization might be questioned, owing to the inter-individual brain differences in terms of Sulci and Gyri, thus an effective registration scheme must be applied to address such a challenge (Kurth et al., 2015).

Compared to other methods of volume analysis, VBM showed to be better than manually traced ROI volume analysis in detecting volumetric changes occurring in the hippocampus in Alzheimer's disease, as well as in differentiating mild to moderate AD subjects from normal controls (Testa et al., 2004). Compared to other methods, detecting hippocampus atrophy like surface based methods including shape analysis, it has been suggested that shape analysis is better than volume analysis in detecting hippocampus atrophy (Maruszak & Thuret, 2014), owing to its ability to foresee Dementia even in the preclinical stages (Achterberg et al., 2013). It was suggested however, that employing both volume and shape anaylsis would have an edge in early predication for Dementia (Achterberg et al., 2013). In another study, comparing different hippocampus changes detection techniques such as voxel based methods, cortical thickness and hippocampus shape analysis, it was proposed that the voxel based techniques and shape analysis performed well in differentiating the AD subjects from normal controls, with higher specificity for the earlier (Cuingnet et al., 2011).

In this study, applied VBM protocol entailed tissue segmentation technique based on AMAP and PVE, as well as spatial normalization technique based on DARTEL were employed, all of which have advantages in reliably detecting hippocampus shrinkage. AMAP has the advantages of considering not only each voxel class type, but also the relationship of each voxel with the neighboring voxels, in another words in can account for the spatial relationship between nearby voxels. Besides,

It employs filtering methods, which account for the MRI signal inhomogeneities, which helps in tissue segmentation even in the presence of random noise and magnetic field intensity non-uniformity (Rajapakse, et al., 1997). PVE has the advantages of considering each voxel as a mixture of 3 tissue classes namely GM, WM and CSF, which helps in a better separation of different tissue type, that might aid in increasing the chances of precise estimation of each tissue volume for further processing steps and for later successful interpretation of the results. As a non-linear transformation approach, DARTEL can correct for the inter-indiviudal brain variability between subjects with regards to the local position, shape and size and thus reliable in studies comparing brain structural changes in multiple subjects (Ashburner, 2007; Ashburner & Friston, 2005). DARTEL has the advantage of performing the normalization while preserving topology (Ripollés et al., 2012), in which the image's deformation during registration is diffeomorphic, invertible and quickly computed (Ashburner, 2007).

Limitations

This study has some limitations. Firstly the handedness in is not sorted as a variable in the ADNI cohort, so it is not regarded as a confounder, inspite of its possible influence on the brain structure (Good et al., 2001). Moreover, subjects in our cohort might be related to each other, and it has been suggested that genetic similarities in related individuals might affect the brain structure (Thompson et al., 2001). Besides, our subjects were scanned in multiple sites and despite the unified protocol that have been implemented and the common post-acquisition quality control to eliminate this effect, this possible confounding effect should be taken into consideration because image dissimilarities caused by technical factors might confound the possible observed disease-related structural changes (Jovicich et al., 2006). ADNI protocol for subjects recruitment in addition was devised to mimic a clinical trial population (Peterson et al., 2001) instead of an actual community population. Consequently our cohort had a high mean education, which was similar in different diagnosis group, which in turn could buffer the observed possible disease-related effect. It should be noted that exact reductions in different hippocampus subregions shouldn't be taken literally because the subregions boundaries might differ with respect to the parcellation/segmentation approach.

In addition, this study results should be compared cautiously with similar studies, due to the difference in sample sizes and the employed VBM steps and algorithms.

Future Aspects

The following aspects could be employed to possibly further add to the study. A Discriminant functional analysis could be done in order to know which hippocampus subregion's mean GMV best classifies the 5 diagnosis groups. In addition, this research can be done on higher hippocampus subregion granularities, in another words the 7 cluster solution on each Hemisphere, parcellated by plachti and colleagues (Plachti et al., 2019). This could help having a closer look on, which specifically the most affected area within each subregion is. This study could be done on a hippocampus model, which could be a consortium of the model based on multi-modal CBP presented by Plachti and colleagues (Plachti et al., 2019), as well as the histological model presented for example by Amunts and colleagues (Amunts et al., 2005), this could be a wider approach in outlining the possible differential affection of the hippocampus along AD progression because it takes into consideration the more conventional histological subfields organization and the relatively newer CBP approach, representing different aspects of hippocampus organization. A future study could add other AD markers in addition to the mean hippocampus GMV such as the CSF markers including beta amyloid (Greene & Killiany, 2012), APOE genes (Fallin et al., 2001), Functional MRI measurement of the blood flow in areas related to memory processing (Machulda et al., 2003), Glucose metabolism measurement by PET scan (Jagust et al., 2009), SPECT measurement of 99mTc-hexamethylpropyleneamine blood flow in certain brain areas (Dougall, Bruggink & Ebmeir, 2004), and Diffusion Tensor Imaging (DTI) measurement of the microscopic structure, represented by water molecule diffusivity, of some brain regions (Chua et al., 2009). Combination of different AD markers in one study could add a thorough view of the possible best marker or best combination of markers in early detecting AD, which possibly will enhance the ability for AD screening at different stages.

Glossary

- Declarative memory: is the gathering of learning experience data as well as facts.
- Episodic memory: subtype of the declarative memory representing memory of personal events.
- Spatial memory as well: memory for the self-location or direction to an object.
- Relational memory: memory relating different components of an experience such as faces and names.
- Explicit memory: explicit remembering of past experiences.
- Encoding: a process, which conveys information perceived into storable memories.
- Consolidation: process of storing labile memories into more stable retrievable ones.
- Recollection: process of remembering of additional information about a specific item.

Abbreviations

AD: Alzheimer's Disease
ADNI: Alzheimer's Disease Neuroimaging Initiative
ADRDA: The Alzheimer's Disease and Related Disorders Association
AMAP: Adaptive Maximum A Posterior
ANCOVA: ANalysis of COVAriance
CAT: Computational Anatomy Toolbox
CBP: Connectivity Based Parcellation
CDR: Clinical Dementia Rating
CN: Cognitively Normal

CSF: Cerebro Spinal Fluid

DARTEL: Diffeomorphic Anatomical Registeration Through Exponentiated Lie algebra

df: degree of freedom

DSM: Diagnostic and Statistical Manual of Mental Disorders

F: F ratio adjusted to the covariates

fMRI: functional Magnetic Resonance Imaging

GDS: Geriatric Depression Scale

GM: Grey Matter

GMV: Grey Matter Volume

GS: Geodesic shooting

LDDMM: Large Deformation Diffeomorphic Metric Mapping

M: Mean

MACM: Meta Analytic Connectivity Modeling

MCI: Mild Cognitive Impairment

mm: mille-meter

MMSE: Mini Mental State Examination

MNI: Montreal Neurological Institute

ms: mille-second

MRI: Magnetic Resonance Imaging

MTL: Medial Temporal Lobe

N: Number of subjects

NINCDS: National Institute of Neurological and Communicative Disorders and Stroke

PCC: Posterior Cingulate Cortex

PFC: PreFrontal Cortex PFC

PVE: Partial Volume Effect

ROI: Region Of Interest

RF: Radio Frequency

RSFC: Resting State Functional Connectivity

SC: Structural Covariance

SD: Standard Deviation

SMCI: Subjective Memory Concern

sMRI: structural Magnetic Resonance Imaging

SPM: Statistic Parametric Mapping

VBM: Voxel Based Morphometry

η^2: effect size

References

Abrahams, S., Morris, R. G., Polkey, C. E., Jarosz, J. M., Cox, T. C. S., Graves, M., & Pickering, A. (1999). Hippocampal Involvement in Spatial and Working Memory: A Structural MRI Analysis of Patients with Unilateral Mesial Temporal Lobe Sclerosis. *Brain and Cognition, 41(1), 39–65.* doi:10.1006/brcg.1999.1095

Achterberg, H. C., van der Lijn, F., den Heijer, T., Vernooij, M. W., Ikram, M. A., Niessen, W. J., & de Bruijne, M. (2013). Hippocampal shape is predictive for the development of dementia in a normal, elderly population*. Human Brain Mapping, 35(5), 2359–2371.* doi:10.1002/hbm.22333

Agosta, F., Vossel, K. A., Miller, B. L., Migliaccio, R., Bonasera, S. J., Filippi, M., … Gorno-Tempini, M. L. (2009). Apolipoprotein E ε4 is associated with disease-specific effects on brain atrophy in Alzheimer's disease and frontotemporal dementia*. Proceedings of the National Academy of Sciences, 106(6), 2018–2022.* doi:10.1073/pnas.0812697106

Amunts, K., Kedo, O., Kindler, M., Pieperhoff, P., Mohlberg, H., Shah, N. J., … Zilles, K. (2005). Cytoarchitectonic mapping of the human amygdala, hippocampal region and entorhinal cortex: intersubject variability and probability maps. *Anatomy and Embryology, 210(5-6), 343–352.* doi:10.1007/s00429-005-0025-5

Apostolova, L. G., Hwang, K. S., Medina, L. D., Green, A. E., Braskie, M. N., Dutton, R. A., … Ringman, J. M. (2011). Cortical and Hippocampal Atrophy in Patients with Autosomal Dominant Familial Alzheimer's Disease*. Dementia and Geriatric Cognitive Disorders, 32(2), 118–125.* doi:10.1159/000330471

Arriagada, P. V., Growdon, J. H., Hedley-Whyte, E. T., & Hyman, B. T. (1992). Neurofibrillary tangles but not senile plaques parallel duration and severity of Alzheimer's disease. *Neurology, 42(3), 631–631.* doi:10.1212/wnl.42.3.631

Ashburner, J. (2007). A fast diffeomorphic image registration algorithm. *NeuroImage, 38(1), 95–113.* doi:10.1016/j.neuroimage.2007.07.007

Ashburner, J. (2012). SPM: A history. *NeuroImage, 62(2), 791–800.* doi:10.1016/j.neuroimage.2011.10.025

Ashburner, J., & Friston, K. J. (2005). Unified segmentation. *NeuroImage, 26(3), 839–851.* doi:10.1016/j.neuroimage.2005.02.018

Baron, J. C., Chételat, G., Desgranges, B., Perchey, G., Landeau, B., de la Sayette, V., & Eustache, F. (2001). In Vivo Mapping of Gray Matter Loss with Voxel-Based Morphometry in Mild Alzheimer's Disease. *NeuroImage, 14(2), 298–309.* doi:10.1006/nimg.2001.0848

Bellec, P., Rosa-Neto, P., Lyttelton, O. C., Benali, H., & Evans, A. C. (2010). Multi-level bootstrap analysis of stable clusters in resting-state fMRI. *NeuroImage, 51(3), 1126–1139.* doi:10.1016/j.neuroimage.2010.02.082

Benson, A. D., Slavin, M. J., Tran, T. T., Petrella, J. R., & Doraiswamy, P. M. (2005). Screening for Early Alzheimer's Disease: Is There Still a Role for the Mini-Mental State Examination? *The Primary Care Companion to The Journal of Clinical Psychiatry,07*(02), 62-67. doi:10.4088/pcc.v07n0204

Bird, C. M., & Burgess, N. (2008). The hippocampus and memory: insights from spatial processing. *Nature Reviews Neuroscience, 9(3), 182–194.* doi:10.1038/nrn2335

Braak, H., & Braak, E. (1991). Neuropathological stageing of Alzheimer-related changes. *Acta Neuropathologica, 82(4), 239–259.* doi:10.1007/bf00308809

Bremner, J. D., Narayan, M., Anderson, E. R., Staib, L. H., Miller, H. L., & Charney, D. S. (2000). Hippocampal Volume Reduction in Major Depression. *American Journal of Psychiatry, 157(1), 115–118.* doi:10.1176/ajp.157.1.115

Brink, T. L. (1984). Limitations of the GDS in cases of pseudodementia. *Clinical Gerontologist: The Journal of Aging and Mental Health, 2*(3), 60-61.

Brown, G. G., Lee, J.-S., Strigo, I. A., Caligiuri, M. P., Meloy, M. J., & Lohr, J. (2011). Voxel-based morphometry of patients with schizophrenia or bipolar I disorder: A matched control study. *Psychiatry Research: Neuroimaging, 194(2), 149–156.* doi:10.1016/j.pscychresns.2011.05.005

Burgess, N., Maguire, E. A., & O'Keefe, J. (2002). The Human Hippocampus and Spatial and Episodic Memory. *Neuron, 35(4), 625–641.* doi:10.1016/s0896-6273(02)00830-9

Campbell, L. E., Daly, E., Toal, F., Stevens, A., Azuma, R., Catani, M., … Murphy, K. C. (2006). Brain and behaviour in children with 22q11.2 deletion syndrome: a volumetric and voxel-based morphometry MRI study. *Brain, 129(5), 1218–1228.*doi:10.1093/brain/awl066

Carmichael, O., Xie, J., Fletcher, E., Singh, B., & DeCarli, C. (2012). Localized hippocampus measures are associated with Alzheimer pathology and cognition independent of total hippocampal volume. *Neurobiology of Aging, 33(6), 1124.e31–1124.e41.* doi:10.1016/j.neurobiolaging.2011.08.016

Chan, D., Fox, N. C., Scahill, R. I., Crum, W. R., Whitwell, J. L., Leschziner, G., … Rossor, M. N. (2001). Patterns of temporal lobe atrophy in semantic dementia and Alzheimer's disease. *Annals of Neurology, 49(4), 433–442.* doi:10.1002/ana.92

Chételat, G., Desgranges, B., Landeau, B., Mezenge, F., Poline, J. B., de la Sayette, V., … Baron, J.-C. (2007). Direct voxel-based comparison between grey matter hypometabolism and atrophy in Alzheimer's disease. *Brain, 131(1), 60–71.* doi:10.1093/brain/awm288

Chételat, G., Desgranges, B., de la Sayette, V., Viader, F., Eustache, F., & Baron, J.-C. (2002). Mapping gray matter loss with voxel-based morphometry in mild cognitive impairment. *NeuroReport, 13(15), 1939–1943.* doi:10.1097/00001756-200210280-00022

Chételat, G., Fouquet, M., Kalpouzos, G., Denghien, I., De la Sayette, V., Viader, F., … Desgranges, B. (2008). Three-dimensional surface mapping of hippocampal atrophy progression from MCI to AD and over normal aging as assessed using voxel-based morphometry. *Neuropsychologia, 46(6), 1721–1731.* doi:10.1016/j.neuropsychologia.2007.11.03

Chételat, G., Landeau, B., Eustache, F., Mézenge, F., Viader, F., de la Sayette, V., … Baron, J.-C. (2005). Using voxel-based morphometry to map the structural changes associated with rapid conversion in MCI: A longitudinal MRI study. *NeuroImage, 27(4), 934–946.* doi:10.1016/j.neuroimage.2005.05.015

Chua, T. C., Wen, W., Chen, X., Kochan, N., Slavin, M. J., Trollor, J. N., … Sachdev, P. S. (2009). Diffusion Tensor Imaging of the Posterior Cingulate is a Useful Biomarker of Mild Cognitive Impairment. The American Journal of Geriatric Psychiatry, 17(7), 602–613. doi:10.1097/jgp.0b013e3181a76e0b

Clark, L. R., Delano-Wood, L., Libon, D. J., McDonald, C. R., Nation, D. A., Bangen, K. J., … Bondi, M. W. (2013). Are Empirically-Derived Subtypes of Mild Cognitive Impairment Consistent with Conventional Subtypes? *Journal of the International Neuropsychological Society, 19(06), 635–645.* doi:10.1017/s1355617713000313

Cohen, N., & Squire, L. (1980). Preserved learning and retention of pattern-analyzing skill in amnesia: dissociation of knowing how and knowing that. *Science, 210(4466), 207–210.* doi:10.1126/science.7414331

Costafreda, S. G., Dinov, I. D., Tu, Z., Shi, Y., Liu, C.-Y., Kloszewska, I., … Simmons, A. (2011). Automated hippocampal shape analysis predicts the onset of dementia in mild cognitive impairment. *NeuroImage, 56(1), 212–219.* doi:10.1016/j.neuroimage.2011.01.050

Cox, R. W. (1996). AFNI: Software for Analysis and Visualization of Functional Magnetic Resonance Neuroimages. *Computers and Biomedical Research, 29(3), 162–173.* doi:10.1006/cbmr.1996.0014

Cuingnet, R., Gerardin, E., Tessieras, J., Auzias, G., Lehéricy, S., Habert, M.-O., … Colliot, O. (2011). Automatic classification of patients with Alzheimer's disease from structural MRI: A comparison of ten methods using the ADNI database. *NeuroImage, 56(2), 766–781.* doi:10.1016/j.neuroimage.2010.06.013

Dawe, B., Procter, A., & Philpot, M. (1992). Concepts of mild memory impairment in the elderly and their relationship to dementia–a review. *International Journal of Geriatric Psychiatry, 7(7), 473–479.* doi:10.1002/gps.930070704

Dempster, A., Laird, N., and Rubin, D. (1977). Maximum likelihood from incomplete data via the EM algorithm. *Journal of the Royal Statistical Society, Series B (Methodological), vol. 39, no. 1, pp. 1ñ38.*

Desikan, R. S., Ségonne, F., Fischl, B., Quinn, B. T., Dickerson, B. C., Blacker, D., … Killiany, R. J. (2006). An automated labeling system for subdividing the human cerebral cortex on MRI scans into gyral based regions of interest. *NeuroImage, 31(3), 968–980.* doi:10.1016/j.neuroimage.2006.01.021

Dickerson, B. C., Goncharova, I., Sullivan, M. P., Forchetti, C., Wilson, R. S., Bennett, D. A., … deToledo-Morrell, L. (2001). MRI-derived entorhinal and hippocampal

atrophy in incipient and very mild Alzheimer's disease ⋆ ⋆This research was supported by grants P01 AG09466 and P30 AG10161 from the National Institute on Aging, National Institutes of Health. *Neurobiology of Aging, 22(5), 747–754.* doi:10.1016/s0197-4580(01)00271-8

Double, K. L., Halliday, G. M., Krill, J. J., Harasty, J. A., Cullen, K., Brooks, W. S., … Broe, G. A. (1996). Topography of brain atrophy during normal aging and alzheimer's disease. *Neurobiology of Aging, 17(4), 513–521.* doi:10.1016/0197-4580(96)00005-x

Dougall, N. J., Bruggink, S., & Ebmeier, K. P. (2004). Systematic Review of the Diagnostic Accuracy of 99mTc-HMPAO-SPECT in Dementia. *American Journal of Geriatric Psychiatry*, *12*(6), 554–570. doi: 10.1097/00019442-200411000-00002

Du, A. T., Schuff, N., Amend, D., Laakso, M. P., Hsu, Y. Y., Jagust, W. J., … Weiner, M. W. (2001). Magnetic resonance imaging of the entorhinal cortex and hippocampus in mild cognitive impairment and Alzheimer's disease. *Journal of neurology, neurosurgery, and psychiatry*, *71*(4), 441–447. doi:10.1136/jnnp.71.4.441

Dubois, B., Feldman, H. H., Jacova, C., DeKosky, S. T., Barberger-Gateau, P., Cummings, J., … Scheltens, P. (2007). Research criteria for the diagnosis of Alzheimer's disease: revising the NINCDS–ADRDA criteria. *The Lancet Neurology, 6(8), 734–746.* doi:10.1016/s1474-4422(07)70178-3

Dubois, B., Feldman, H. H., Jacova, C., Cummings, J. L., DeKosky, S. T., Barberger-Gateau, P., … Scheltens, P. (2010). Revising the definition of Alzheimer's disease: a new lexicon. *The Lancet Neurology, 9(11), 1118–1127.* doi:10.1016/s1474-4422(10)70223-4

Dubois, B., Feldman, H. H., Jacova, C., Hampel, H., Molinuevo, J. L., Blennow, K., … Cummings, J. L. (2014). Advancing research diagnostic criteria for Alzheimer's

disease: the IWG-2 criteria. *The Lancet Neurology, 13(6), 614–629.* doi:10.1016/s1474-4422(14)70090-0

Echávarri, C., Aalten, P., Uylings, H. B. M., Jacobs, H. I. L., Visser, P. J., Gronenschild, E. H. B. M., … Burgmans, S. (2010). Atrophy in the parahippocampal gyrus as an early biomarker of Alzheimer's disease. *Brain Structure and Function, 215(3-4), 265–271.* doi:10.1007/s00429-010-0283-8

Eichenbaum H., Cohen N. J. (2001). From Conditioning to Conscious Recollection: Memory Systems of the Brain. *Oxford psychology series; no. 35*, *New York, NY, US: Oxford University Press.* doi:10.1093/acprof:oso/9780195178043.001.0001

Eichenbaum, H., Otto, T., & Cohen, N. J. (1992). The hippocampus—what does it do? *Behavioral and Neural Biology, 57(1), 2–36.* doi:10.1016/0163-1047(92)90724-i

Eichenbaum, H. (1999). The hippocampus and mechanisms of declarative memory. *Behavioural Brain Research, 103(2), 123–133.* doi:10.1016/s0166-4328(99)00044-3

Eickhoff, S. B., Bzdok, D., Laird, A. R., Roski, C., Caspers, S., Zilles, K., & Fox, P. T. (2011). Co-activation patterns distinguish cortical modules, their connectivity and functional differentiation. *NeuroImage, 57(3), 938–949.* doi:10.1016/j.neuroimage.2011.05.021

Eickhoff, S. B., Thirion, B., Varoquaux, G., & Bzdok, D. (2015). Connectivity-based parcellation: Critique and implications. *Human Brain Mapping, 36(12), 4771–4792.* doi:10.1002/hbm.22933

Eickhoff, S. B., Stephan, K. E., Mohlberg, H., Grefkes, C., Fink, G. R., Amunts, K., & Zilles, K. (2005). A new SPM toolbox for combining probabilistic cytoarchitectonic maps and functional imaging data. *NeuroImage, 25(4), 1325–1335.* doi:10.1016/j.neuroimage.2004.12.034

Eickhoff, S. B., Yeo, B. T. T., & Genon, S. (2018). Imaging-based parcellations of the human brain. *Nature Reviews Neuroscience.* doi:10.1038/s41583-018-0071-7

Fallin, D., Cohen, A., Essioux, L., Chumakov, I., Blumenfeld, M., Cohen, D., & Schork, N. J. (2001). Genetic analysis of case/control data using estimated haplotype frequencies: application to APOE locus variation and Alzheimer's disease. *Genome research*, *11*(1), 143–151. doi:10.1101/gr.148401

Fanselow, M. S., & Dong, H. W. (2010). Are the dorsal and ventral hippocampus functionally distinct structures? *Neuron*, *65*(1), 7–19. doi:10.1016/j.neuron.2009.11.031

Flicker, C., Ferris, S. H., & Reisberg, B. (1991). Mild cognitive impairment in the elderly: Predictors of dementia. *Neurology, 41(7), 1006–1006.* doi:10.1212/wnl.41.7.1006

Folstein, M. F., Folstein, S. E., & McHugh, P. R. (1975). "Mini-mental state". *Journal of Psychiatric Research, 12(3), 189–198.* doi:10.1016/0022-3956(75)90026-6

Fox, N. C., Scahill, R. I., Crum, W. R., & Rossor, M. N. (1999). Correlation between rates of brain atrophy and cognitive decline in AD. *Neurology, 52(8), 1687–1687.* doi:10.1212/wnl.52.8.1687

Fox, N. C., Warrington, E. K., Freeborough, P. A., Hartikainen, P., Kennedy, A. M., Stevens, J. M., & Rossor, M. N. (1996). Presymptomatic hippocampal atrophy in Alzheimer's disease. *Brain, 119(6), 2001–2007.* doi:10.1093/brain/119.6.2001

Frankó, E., Joly, O., & Alzheimer's Disease Neuroimaging Initiative (2013). Evaluating Alzheimer's disease progression using rate of regional hippocampal atrophy. *PloS one*, *8*(8), e71354. doi:10.1371/journal.pone.0071354

Frisoni, G. B., Bocchetta, M., Chetelat, G., Rabinovici, G. D., de Leon, M. J., … Kaye, J. (2013). Imaging markers for Alzheimer disease: Which vs how. *Neurology, 81(5), 487–500.* doi:10.1212/wnl.0b013e31829d86e8

Frisoni, G. B., Fox, N. C., Jack, C. R., Scheltens, P., & Thompson, P. M. (2010). The clinical use of structural MRI in Alzheimer disease. *Nature Reviews Neurology, 6(2), 67–77.*doi:10.1038/nrneurol.2009.215

Frisoni, G. B., Testa, C., Zorzan, A., Sabattoli, F., Beltramello, A., Soininen, H., & Laakso, M. P. (2002). Detection of grey matter loss in mild Alzheimer's disease with voxel based morphometry. *Journal of neurology, neurosurgery, and psychiatry*, *73*(6), 657–664. doi:10.1136/jnnp.73.6.657

Genon, S., Reid, A., Langner, R., Amunts, K., & Eickhoff, S. B. (2018). How to Characterize the Function of a Brain Region. *Trends in Cognitive Sciences, 22(4), 350–364.* doi:10.1016/j.tics.2018.01.010

Good, C. D., Johnsrude, I. S., Ashburner, J., Henson, R. N. A., Friston, K. J., & Frackowiak, R. S. J. (2001). A Voxel-Based Morphometric Study of Ageing in 465 Normal Adult Human Brains*. NeuroImage, 14(1), 21–36.* doi:10.1006/nimg.2001.0786

Gordon, B. A., Blazey, T., Benzinger, T. L. S., & Head, D. (2013). Effects of Aging and Alzheimer's Disease Along the Longitudinal Axis of the Hippocampus. *Journal of Alzheimer's Disease, 37(1), 41–50.* doi:10.3233/jad-130011

Grady, C. L., McIntosh, A. R., & Craik, F. I. M. (2003). Age-related differences in the functional connectivity of the hippocampus during memory encoding. *Hippocampus, 13(5), 572–586.* doi:10.1002/hipo.10114

Grand, J. H., Caspar, S., & Macdonald, S. W. (2011). Clinical features and multidisciplinary approaches to dementia care. *Journal of multidisciplinary healthcare*, *4*, 125–147. doi:10.2147/JMDH.S17773

Greene, S. J., & Killiany, R. J. (2011). Hippocampal Subregions are Differentially Affected in the Progression to Alzheimer's Disease. *The Anatomical Record: Advances in Integrative Anatomy and Evolutionary Biology, 295(1), 132–140.* doi:10.1002/ar.21493

Gunter, J. L., Borowski, B. J., Thostenson, K., Arani, A., Reid, R. I., Cash, D. M., … Jack, C. R. (2017). ADNI-3 MRI PROTOCOL. *Alzheimer's & Dementia, 13(7), P104–P105.* doi:10.1016/j.jalz.2017.06.2411

Guo, X., Wang, Z., Li, K., Li, Z., Qi, Z., Jin, Z., … Chen, K. (2010). Voxel-based assessment of gray and white matter volumes in Alzheimer's disease. *Neuroscience letters*, *468*(2), 146–150. doi:10.1016/j.neulet.2009.10.086

Guo, Y., Zhang, Z., Zhou, B., Wang, P., Yao, H., Yuan, M., … Liu, Y. (2014). Grey-matter volume as a potential feature for the classification of Alzheimer's disease and mild cognitive impairment: an exploratory study. *Neuroscience Bulletin, 30(3), 477–489.* doi:10.1007/s12264-013-1432-x

Gupta, M. & Chen, Y. (2010) Theory and Use of the EM Algorithm. *Foundations and Trends in Signal Processing, Vol. 4, No. 3 223–296*. doi :10.1561/2000000034

Hancock, P., & Larner, A. J. (2010). Test Your Memory test: diagnostic utility in a memory clinic population. *International Journal of Geriatric Psychiatry, 26(9), 976–980.* doi:10.1002/gps.2639

Held, K., Kops, E. R., Krause, B. J., Wells, W. M., Kikinis, R., & Muller-Gartner, H.W. (1997). Markov random field segmentation of brain MR images. *IEEE Transactions on Medical Imaging, 16(6), 878–886* .doi:10.1109/42.650883

Hirata, Y., Matsuda, H., Nemoto, K., Ohnishi, T., Hirao, K., Yamashita, F., … Samejima, H. (2005). *Voxel-based morphometry to discriminate early Alzheimer's disease*

from controls. Neuroscience Letters, 382(3), 269–274. doi:10.1016/j.neulet.2005.03.038

Horner, A. J., & Doeller, C. F. (2017). Plasticity of hippocampal memories in humans. *Current Opinion in Neurobiology, 43, 102–109.* doi:10.1016/j.conb.2017.02.004

Hua, X., Leiv, A., Lee, S., Klunder, A., Toga, A., Lepore, N., … Barysheva, M. (2008). 3D characterization of brain atrophy in Alzheimer's disease and mild cognitive impairment using tensor-based morphometry. *NeuroImage, 41(1), 19–34.* doi:10.1016/j.neuroimage.2008.02.010

Hua, X., Lee, S., Hibar, D. P., Yanovsky, I., Leow, A. D., Toga, A. W., … Thompson, P. M. (2010). Mapping Alzheimer's disease progression in 1309 MRI scans: Power estimates for different inter-scan intervals. *NeuroImage, 51(1), 63–75.* doi:10.1016/j.neuroimage.2010.01.104

Hutsler, J., & Galuske, R. A. (2003). Hemispheric asymmetries in cerebral cortical networks. *Trends in Neurosciences,26*(8), 429-435. doi:10.1016/s0166-2236(03)00198-x

Iseki, E., Murayama, N., Yamamoto, R., Fujishiro, H., Suzuki, M., Kawano, M., … Sato, K. (2010). Construction of a18F-FDG PET normative database of Japanese healthy elderly subjects and its application to demented and mild cognitive impairment patients. *International Journal of Geriatric Psychiatry, 25(4), 352–361.* doi:10.1002/gps.2346

Jack, C. R., Albert, M. S., Knopman, D. S., McKhann, G. M., Sperling, R. A., Carrillo, M. C., … Phelps, C. H. (2011). Introduction to the recommendations from the National Institute on Aging-Alzheimer's Association workgroups on diagnostic guidelines for Alzheimer's disease. *Alzheimer's & Dementia, 7(3), 257–262.* doi:10.1016/j.jalz.2011.03.004

Jack, C. R., Bernstein, M. A., Borowski, B. J., Gunter, J. L., Fox, N. C., Thompson, P. M., … Weiner, M. W. (2010). Update on the Magnetic Resonance Imaging core of the Alzheimer's Disease Neuroimaging Initiative*. Alzheimer's & Dementia, 6(3), 212–220.* doi:10.1016/j.jalz.2010.03.004

Jack, C. R., Jr, Bernstein, M. A., Fox, N. C., Thompson, P., Alexander, G., Harvey, D., … Weiner, M. W. (2008). The Alzheimer's Disease Neuroimaging Initiative (ADNI): MRI methods. *Journal of magnetic resonance imaging : JMRI*, *27*(4), 685–691. doi:10.1002/jmri.21049

Jack, C. R., Knopman, D. S., Jagust, W. J., Petersen, R. C., Weiner, M. W., Aisen, P. S., . . . Trojanowski, J. Q. (2013). Tracking pathophysiological processes in Alzheimers disease: An updated hypothetical model of dynamic biomarkers. *The Lancet Neurology,12*(2), 207-216. doi:10.1016/s1474-4422(12)70291-0

Jack, C. R., Petersen, R. C., O'Brien, P. C., & Tangalos, E. G. (1992). MR-based hippocampal volumetry in the diagnosis of Alzheimer's disease*. Neurology, 42(1), 183–183.* doi:10.1212/wnl.42.1.183

Jack, C. R., Petersen, R. C., Xu, Y. C., Waring, S. C., O'Brien, P. C., Tangalos, E. G., … Kokmen, E. (1997). Medial temporal atrophy on MRI in normal aging and very mild Alzheimer's disease. *Neurology, 49(3), 786–794.* doi:10.1212/wnl.49.3.786

Jack, C. R., Jr, Petersen, R. C., Xu, Y. C., O'Brien, P. C., Smith, G. E., Ivnik, R. J., … Kokmen, E. (1999). Prediction of AD with MRI-based hippocampal volume in mild cognitive impairment. *Neurology*, *52*(7), 1397–1403. doi:10.1212/wnl.52.7.1397

Jagust, W. J., Landau, S. M., Shaw, L. M., Trojanowski, J. Q., Koeppe, R. A., … Reiman, E. M. (2009). Relationships between biomarkers in aging and dementia. Neurology, 73(15), 1193–1199. doi:10.1212/wnl.0b013e3181bc010c

Jenkinson, M., Beckmann, C. F., Behrens, T. E. J., Woolrich, M. W., & Smith, S. M.

(2012). FSL. *NeuroImage, 62(2), 782–790.* doi:10.1016/j.neuroimage.2011.09.015

Jessen, F. (2010). Prediction of Dementia by Subjective Memory Impairment: Effects of Severity and Temporal Association With Cognitive Impairment. *Archives of General Psychiatry, 67(4), 414.* doi:10.1001/archgenpsychiatry.2010.30

Jessen, F., Wolfsgruber, S., Wiese, B., Bickel, H., Mösch, E., Kaduszkiewicz, H., … Wagner, M. (2014). AD dementia risk in late MCI, in early MCI, and in subjective memory impairment. *Alzheimer's & Dementia, 10(1), 76–83.* doi:10.1016/j.jalz.2012.09.017

Jicha, G. A., Parisi, J. E., Dickson, D. W., Johnson, K., Cha, R., Ivnik, R. J., … Petersen, R. C. (2006). Neuropathologic Outcome of Mild Cognitive Impairment Following Progression to Clinical Dementia. *Archives of Neurology, 63(5), 674.* doi:10.1001/archneur.63.5.674

Johnson, K. A., Fox, N. C., Sperling, R. A., & Klunk, W. E. (2012). *Brain Imaging in Alzheimer Disease. Cold Spring Harbor Perspectives in Medicine, 2(4), a006213–a006213.*doi:10.1101/cshperspect.a006213

Jovicich, J., Czanner, S., Greve, D., Haley, E., van der Kouwe, A., Gollub, R., … Dale, A. (2006). Reliability in multi-site structural MRI studies: Effects of gradient non-linearity correction on phantom and human data. *NeuroImage, 30(2), 436–443.* doi:10.1016/j.neuroimage.2005.09.046

Karas, G. B., Burton, E. J., Rombouts, S. A. R. B., van Schijndel, R. A., O'Brien, J. T., Scheltens, P. h., … Barkhof, F. (2003). A comprehensive study of gray matter loss in patients with Alzheimer's disease using optimized voxel-based morphometry. *NeuroImage, 18(4), 895–907.* doi:10.1016/s1053-8119(03)00041-7

Karas, G. B., Scheltens, P., Rombouts, S. A. R. B., Visser, P. J., van Schijndel, R. A., Fox, N. C., & Barkhof, F. (2004). Global and local gray matter loss in mild cognitive impairment and Alzheimer's disease. *NeuroImage, 23(2), 708–716.* doi:10.1016/j.neuroimage.2004.07.006

Kawai, Y., Miura, R., Tsujimoto, M., Sakurai, T., Yamaoka, A., Takeda, A., … Toba, K. (2013). Neuropsychological differentiation between Alzheimer's disease and dementia with Lewy bodies in a memory clinic*. Psychogeriatrics, 13(3), 157–163.* doi:10.1111/psyg.12019

Khan, T. K. (2016). Clinical Diagnosis of Alzheimer's Disease*. Biomarkers in Alzheimer's Disease, 27–48.* doi:10.1016/b978-0-12-804832-0.00002-x

Kinno, R., Shiromaru, A., Mori, Y., Futamura, A., Kuroda, T., Yano, S., … Ono, K. (2017). Differential Effects of the Factor Structure of the Wechsler Memory Scale-Revised on the Cortical Thickness and Complexity of Patients Aged Over 75 Years in a Memory Clinic Setting*. Frontiers in Aging Neuroscience, 9.* doi:10.3389/fnagi.2017.00405

Komorowski, R. W., Garcia, C. G., Wilson, A., Hattori, S., Howard, M. W., & Eichenbaum, H. (2013). Ventral Hippocampal Neurons Are Shaped by Experience to Represent Behaviorally Relevant Contexts*. Journal of Neuroscience, 33(18), 8079–8087.* doi:10.1523/jneurosci.5458-12.2013

Konkel, A. (2009). Relational memory and the hippocampus: Representations and methods. *Frontiers in Neuroscience, 3(2), 166–174.* doi:10.3389/neuro.01.023.2009

Kurth, F., Luders, E., & Gaser, C. (2015). Voxel-Based Morphometry*. Brain Mapping, 345–349.* doi:10.1016/b978-0-12-397025-1.00304-3

Laakso, M. P., Frisoni, G. B., Könönen, M., Mikkonen, M., Beltramello, A., Geroldi, C., … Aronen, H. J. (2000). Hippocampus and entorhinal cortex in frontotemporal

dementia and Alzheimer's disease: a morphometric MRI study. *Biological Psychiatry, 47(12), 1056–1063.* doi:10.1016/s0006-3223(99)00306-6

Lüdeke, K. M., Röschmann, P., & Tischler, R. (1985). Susceptibility artefacts in NMR imaging. *Magnetic Resonance Imaging, 3(4), 329–343.* doi:10.1016/0730-725x(85)90397-2

Machulda, M. M., Ward, H. A., Borowski, B., Gunter, J. L., Cha, R. H., O'Brien, P. C., … Jack, C. R. (2003). Comparison of memory fMRI response among normal, MCI, and Alzheimer's patients. Neurology, 61(4), 500–506. doi:10.1212/01.wnl.0000079052.01016.78

Maguire, E. A., Burgess, N., & O'Keefe, J. (1999). Human spatial navigation: cognitive maps, sexual dimorphism, and neural substrates. *Current Opinion in Neurobiology, 9(2), 171–177.* doi:10.1016/s0959-4388(99)80023-3

Martin, S. B., Smith, C. D., Collins, H. R., Schmitt, F. A., & Gold, B. T. (2010). Evidence that volume of anterior medial temporal lobe is reduced in seniors destined for mild cognitive impairment. *Neurobiology of Aging, 31(7), 1099–1106.* doi:10.1016/j.neurobiolaging.2008.08.010

Maruszak, A., & Thuret, S. (2014). Why looking at the whole hippocampus is not enough - a critical role for anteroposterior axis, subfield and activation analyses to enhance predictive value of hippocampal changes for Alzheimer's disease diagnosis. *Frontiers in Cellular Neuroscience, 8*. doi:10.3389/fncel.2014.00095

McKhann, G., Drachman, D., Folstein, M., Katzman, R., Price, D., & Stadlan, E. M. (1984). Clinical diagnosis of Alzheimer's disease: Report of the NINCDS-ADRDA Work Group* under the auspices of Department of Health and Human Services Task Force on Alzheimer's Disease. *Neurology, 34(7), 939–939.* doi:10.1212/wnl.34.7.939

McKhann, G. M., Knopman, D. S., Chertkow, H., Hyman, B. T., Jack, C. R., Kawas, C. H., … Phelps, C. H. (2011). The diagnosis of dementia due to Alzheimer's disease: Recommendations from the National Institute on Aging-Alzheimer's Association workgroups on diagnostic guidelines for Alzheimer's disease. *Alzheimer's & Dementia, 7(3), 263–269.* doi:10.1016/j.jalz.2011.03.005

Mechelli, A., Price, C., Friston, K., & Ashburner, J. (2005). Voxel-Based Morphometry of the Human Brain: Methods and Applications. *Current Medical Imaging Reviews, 1(2), 105–113.* doi:10.2174/1573405054038726

Meisenzahl, E. M., Koutsouleris, N., Bottlender, R., Scheuerecker, J., Jäger, M., Teipel, S. J., … Möller, H.-J. (2008). Structural brain alterations at different stages of schizophrenia: A voxel-based morphometric study. *Schizophrenia Research, 104(1-3), 44–60.* doi:10.1016/j.schres.2008.06.023

Mendonça, M. D., Alves, L., & Bugalho, P. (2015). From Subjective Cognitive Complaints to Dementia: Who Is at Risk?: A Systematic Review. *American Journal of Alzheimer's Disease & Other Dementiasr, 31(2), 105–114.* doi:10.1177/1533317515592331

Miranda, A. M., Bravo, F. V., Chan, R. B., Sousa, N., Di Paolo, G., & Oliveira, T. G. (2019). Differential lipid composition and regulation along the hippocampal longitudinal axis. Translational Psychiatry, 9(1). doi:10.1038/s41398-019-0478-6

Mitchell, A. J. (2009). A meta-analysis of the accuracy of the mini-mental state examination in the detection of dementia and mild cognitive impairment. *Journal of Psychiatric Research, 43(4), 411–431.* doi:10.1016/j.jpsychires.2008.04.014

Moon, S. W., Lee, B., & Choi, Y. C. (2018). Changes in the Hippocampal Volume and Shape in Early-Onset Mild Cognitive Impairment. *Psychiatry investigation*, *15*(5), 531–537. doi:10.30773/pi.2018.02.12

Morris, J. C. (1993). The Clinical Dementia Rating (CDR): Current version and scoring rules. *Neurology, 43(11), 2412–2412.* doi:10.1212/wnl.43.11.2412-a

Morris, J. C., McKeel, D. W., Fulling, K., Torack, R. M., & Berg, L. (1988). Validation of clinical diagnostic criteria for Alzheimer's disease. *Annals of Neurology, 24(1), 17–22.* doi:10.1002/ana.410240105

Morris, J. C., Storandt, M., Miller, J. P., McKeel, D. W., Price, J. L., Rubin, E. H., & Berg, L. (2001). Mild Cognitive Impairment Represents Early-Stage Alzheimer Disease. *Archives of Neurology, 58(3).* doi:10.1001/archneur.58.3.397

Moser, M.-B., & Moser, E. I. (1998). Functional differentiation in the hippocampus. *Hippocampus, 8(6), 608–619.* doi:10.1002/(sici)1098-1063(1998)8:63.0.co;2-7

Nadel, L., & Moscovitch, M. (1997). Memory consolidation, retrograde amnesia and the hippocampal complex. *Current Opinion in Neurobiology, 7(2), 217–227.* doi:10.1016/s0959-4388(97)80010-4

Narayana, P. A., Brey, W. W., Kulkarni, M. V., & Sievenpiper, C. L. (1988). Compensation for surface coil sensitivity variation in magnetic resonance imaging. *Magnetic Resonance Imaging, 6(3), 271–274.* doi:10.1016/0730-725x(88)90401-8

Ouchi, Y., Nobezawa, S., Okada, H., Yoshikawa, E., Futatsubashi, M., & Kaneko, M. (1998). Altered glucose metabolism in the hippocampal head in memory impairment. *Neurology, 51(1), 136–142.*doi:10.1212/wnl.51.1.136

Pedraza, O., Bowers, D., & Gilmore, R. (2004). Asymmetry of the hippocampus and amygdala in MRI volumetric measurements of normal adults. *Journal of the International Neuropsychological Society, 10(05).* doi:10.1017/s1355617704105080

Peixoto-Santos, J. E., Carvalho, L. E. D. de, Kandratavicius, L., Diniz, P. R. B., Scandiuzzi, R. C., Coras, R., … Leite, J. P. (2018). Manual Hippocampal Subfield Segmentation Using High-Field MRI: Impact of Different Subfields in Hippocampal Volume Loss of Temporal Lobe Epilepsy Patients. *Frontiers in Neurology, 9.* doi:10.3389/fneur.2018.00927

Pennanen, C. (2005). A voxel based morphometry study on mild cognitive impairment. *Journal of Neurology, Neurosurgery & Psychiatry, 76(1), 11–14.* doi:10.1136/jnnp.2004.035600

Petersen, R. C., Aisen, P. S., Beckett, L. A., Donohue, M. C., Gamst, A. C., Harvey, D. J., … Weiner, M. W. (2009). Alzheimer's Disease Neuroimaging Initiative (ADNI): Clinical characterization. *Neurology, 74(3), 201–209.* doi:10.1212/wnl.0b013e3181cb3e25

Petersen, R. C., Doody, R., Kurz, A., Mohs, R. C., Morris, J. C., Rabins, P. V., … Winblad, B. (2001). Current Concepts in Mild Cognitive Impairment. *Archives of Neurology, 58(12), 1985.* doi:10.1001/archneur.58.12.1985

Petersen, R. C., Smith, G. E., Waring, S. C., Ivnik, R. J., Tangalos, E. G., & Kokmen, E. (1999). Mild Cognitive Impairment. *Archives of Neurology, 56(3), 303.* doi:10.1001/archneur.56.3.303

Plachti, A., Eickhoff, S. B., Hoffstaedter, F., Patil, K. R., Laird, A. R., Fox, P. T., ... Genon, S. (2019). Multimodal Parcellations and Extensive Behavioral Profiling Tackling the Hippocampus Gradient. *Cerebral Cortex*. https://doi.org/10.1093/cercor/bhy336.

Prince, S. E. (2005). Neural Correlates of Relational Memory: Successful Encoding and Retrieval of Semantic and Perceptual Associations. *Journal of Neuroscience, 25(5), 1203–1210.* doi:10.1523/jneurosci.2540-04.2005

Pluta, J., Yushkevich, P., Das, S., & Wolk, D. (2012). In vivo Analysis of Hippocampal Subfield Atrophy in Mild Cognitive Impairment via Semi-Automatic Segmentation of T2-Weighted MRI. *Journal of Alzheimer's Disease, 31(1), 85–99.* doi:10.3233/jad-2012-111931

Raji, C. A., Lopez, O. L., Kuller, L. H., Carmichael, O. T., & Becker, J. T. (2009). Age, Alzheimer disease, and brain structure. *Neurology, 73(22), 1899–1905.* doi:10.1212/wnl.0b013e3181c3f293

Rajapakse, J. C., Giedd, J. N., & Rapoport, J. L. (1997). Statistical approach to segmentation of single-channel cerebral MR images*. IEEE Transactions on Medical Imaging, 16(2), 176–186.* doi:10.1109/42.563663

Reisberg, B., Shulman, M. B., Torossian, C., Leng, L., & Zhu, W. (2010). Outcome over seven years of healthy adults with and without subjective cognitive impairment*. Alzheimer's & Dementia, 6(1), 11–24.* doi:10.1016/j.jalz.2009.10.002

Ridha, B. H., Barnes, J., Bartlett, J. W., Godbolt, A., Pepple, T., Rossor, M. N., & Fox, N. C. (2006). Tracking atrophy progression in familial Alzheimer's disease: a serial MRI study. *The Lancet Neurology, 5(10), 828–834.* doi:10.1016/s1474-4422(06)70550-6

Ripollés, P., Marco-Pallarés, J., de Diego-Balaguer, R., Miró, J., Falip, M., Juncadella, M., … Rodriguez-Fornells, A. (2012). *Analysis of automated methods for spatial normalization of lesioned brains. NeuroImage, 60(2), 1296–1306.* doi:10.1016/j.neuroimage.2012.01.094

Robinson, J. L., Barron, D. S., Kirby, L. A., Bottenhorn, K. L., Hill, A. C., Murphy, J. E., … Fox, P. T. (2015). Neurofunctional topography of the human hippocampus. *Human brain mapping*, *36*(12), 5018–5037. doi:10.1002/hbm.22987

Rosen, W. G., Terry, R. D., Fuld, P. A., Katzman, R., & Peck, A. (1980). Pathological verification of ischemic score in differentiation of dementias. *Annals of Neurology, 7(5), 486–488.* doi: 10.1002/ana.410070516

Rubin, R., Schwarb, H., Lucas, H., Dulas, M., & Cohen, N. (2017). Dynamic Hippocampal and Prefrontal Contributions to Memory Processes and Representations Blur the Boundaries of Traditional Cognitive Domains. *Brain Sciences,7*(12), 82. doi:10.3390/brainsci7070082

Scheltens, P., Barkhof, F., Leys, D., Wolters, E. C., Ravid, R., & Kamphorst, W. (1995). Histopathologic correlates of white matter changes on MRI in Alzheimer's disease and normal aging. *Neurology, 45(5), 883–888.* doi:10.1212/wnl.45.5.883

Schuff, N., Woerner, N., Boreta, L., Kornfield, T., Shaw, L. M., Trojanowski, J. Q., … Alzheimer's Disease Neuroimaging Initiative (2009). MRI of hippocampal volume loss in early Alzheimer's disease in relation to ApoE genotype and biomarkers. *Brain : a journal of neurology*, *132*(Pt 4), 1067–1077. doi:10.1093/brain/awp007

Scoville, W. B., & Milner, B. (1957). Loss of recent memory after bilateral hippocampal lesions. *Journal of neurology, neurosurgery, and psychiatry*, *20*(1), 11–21. doi:10.1136/jnnp.20.1.11

Shah, P. J., Ebmeier, K. P., Glabus, M. F., & Goodwin, G. M. (1998). Cortical grey matter reductions associated with treatment-resistant chronic unipolar depression. *British Journal of Psychiatry, 172(06), 527–532.* doi: 10.1192/bjp.172.6.527

Sheikh, J. I., & Yesavage, J. A. (1986). Geriatric Depression Scale (GDS): Recent evidence and development of a shorter version. *Clinical Gerontologist: The Journal of Aging and Mental Health, 5*(1-2), 165-173. http://dx.doi.org/10.1300/J018v05n01_09

Shi, F., Liu, B., Zhou, Y., Yu, C., & Jiang, T. (2009). Hippocampal volume and asymmetry in mild cognitive impairment and Alzheimer's disease: Meta-analyses of MRI studies. *Hippocampus, 19(11), 1055–1064.* doi:10.1002/hipo.20573

Shipton, O. A., El-Gaby, M., Apergis-Schoute, J., Deisseroth, K., Bannerman, D. M., Paulsen, O., & Kohl, M. M. (2014). Left–right dissociation of hippocampal memory processes in mice. *Proceedings of the National Academy of Sciences,111(42), 15238-15243.* doi:10.1073/pnas.1405648111

Silani, G., Frith, U., Demonet, J.-F., Fazio, F., Perani, D., Price, C., … Paulesu, E. (2005). Brain abnormalities underlying altered activation in dyslexia: a voxel based morphometry study. *Brain, 128(10), 2453–2461.* doi:10.1093/brain/awh579

Sled, J. G., Zijdenbos, A. P., & Evans, A. C. (1998). A nonparametric method for automatic correction of intensity nonuniformity in MRI data. *IEEE Transactions on Medical Imaging, 17(1), 87–97.* doi:10.1109/42.668698

Smith, C. D., Chebrolu, H., Wekstein, D. R., Schmitt, F. A., & Markesbery, W. R. (2007). Age and gender effects on human brain anatomy: A voxel-based morphometric study in healthy elderly. *Neurobiology of Aging, 28(7), 1075–1087.* doi:10.1016/j.neurobiolaging.2006.05.018

Smith, S. M., Jenkinson, M., Woolrich, M. W., Beckmann, C. F., Behrens, T. E. J., Johansen-Berg, H., … Matthews, P. M. (2004). Advances in functional and structural MR image analysis and implementation as FSL. *NeuroImage, 23, S208–S219.* doi:10.1016/j.neuroimage.2004.07.051

Sperling, R. A., Aisen, P. S., Beckett, L. A., Bennett, D. A., Craft, S., Fagan, A. M., … Phelps, C. H. (2011). Toward defining the preclinical stages of Alzheimer's disease: Recommendations from the National Institute on Aging-Alzheimer's

Association workgroups on diagnostic guidelines for Alzheimer's disease. *Alzheimer's & Dementia, 7(3), 280–292.* doi:10.1016/j.jalz.2011.03.003

Squire, L. R., Genzel, L., Wixted, J. T., & Morris, R. G. (2015). Memory Consolidation. *Cold Spring Harbor Perspectives in Biology, 7(8), a021766.* doi:10.1101/cshperspect.a021766

Stonnington, C. M., Tan, G., Klöppel, S., Chu, C., Draganski, B., Jack, C. R., … Frackowiak, R. S. J. (2008). Interpreting scan data acquired from multiple scanners: A study with Alzheimer's disease. *NeuroImage, 39(3), 1180–1185.* doi: 10.1016/j.neuroimage.2007.09.066

Storandt, M., Grant, E. A., Miller, J. P., & Morris, J. C. (2006). Longitudinal course and neuropathologic outcomes in original vs revised MCI and in pre-MCI. *Neurology, 67(3), 467–473.* doi:10.1212/01.wnl.0000228231.26111.6e

Striepens, N., Scheef, L., Wind, A., Popp, J., Spottke, A., Cooper-Mahkorn, D., … Jessen, F. (2010). Volume Loss of the Medial Temporal Lobe Structures in Subjective Memory Impairment. *Dementia and Geriatric Cognitive Disorders, 29(1), 75–81.* doi:10.1159/000264630

Testa, C., Laakso, M. P., Sabattoli, F., Rossi, R., Beltramello, A., Soininen, H., & Frisoni, G. B. (2004). A comparison between the accuracy of voxel-based morphometry and hippocampal volumetry in Alzheimer's disease. *Journal of Magnetic Resonance Imaging, 19(3), 274–282.* doi:10.1002/jmri.20001

Thompson, P. M., Cannon, T. D., Narr, K. L., van Erp, T., Poutanen, V.-P., Huttunen, M., … Toga, A. W. (2001). Genetic influences on brain structure. Nature Neuroscience, 4(12), 1253–1258. doi:10.1038/nn758

Tohka, J., Zijdenbos, A., & Evans, A. (2004). Fast and robust parameter estimation for statistical partial volume models in brain MRI. *NeuroImage, 23(1), 84–97.* doi:10.1016/j.neuroimage.2004.05.007

Tulving, E. (2002). Episodic Memory: From Mind to Brain. *Annual Review of Psychology, 53(1), 1–25.* doi:10.1146/annurev.psych.53.100901.135

Uğurbil, K., Xu, J., Auerbach, E. J., Moeller, S., Vu, A. T., Duarte-Carvajalino, J. M., … Yacoub, E. (2013). Pushing spatial and temporal resolution for functional and diffusion MRI in the Human Connectome Project. *NeuroImage, 80, 80–104.* doi:10.1016/j.neuroimage.2013.05.012

Uylings, H. B. M., & de Brabander, J. M. (2002). Neuronal Changes in Normal Human Aging and Alzheimer's Disease. *Brain and Cognition, 49(3), 268–276.* doi:10.1006/brcg.2001.1500

Van Leemput, K., Bakkour, A., Benner, T., Wiggins, G., Wald, L. L., Augustinack, J., … Fischl, B. (2009). Automated segmentation of hippocampal subfields from ultra-high resolution in vivo MRI. *Hippocampus, 19(6), 549–557.* doi:10.1002/hipo.20615

Vargha-Khadem, F. (1997). Differential Effects of Early Hippocampal Pathology on Episodic and Semantic Memory. *Science, 277(5324), 376–380.* doi:10.1126/science.277.5324.376

Vemuri, P., & Jack, C. R. (2010). Role of structural MRI in Alzheimer's disease. *Alzheimer's Research & Therapy, 2(4), 23.* doi:10.1186/alzrt47

Vemuri, P., Wiste, H. J., Weigand, S. D., Shaw, L. M., Trojanowski, J. Q., … Weiner, M. W. (2009). MRI and CSF biomarkers in normal, MCI, and AD subjects: Diagnostic discrimination and cognitive correlations. *Neurology, 73(4), 287–293.* doi:10.1212/wnl.0b013e3181af79e5

Viard, A., Piolino, P., Desgranges, B., Chételat, G., Lebreton, K., Landeau, B., … Eustache, F. (2007). Hippocampal activation for autobiographical memories over the entire lifetime in healthy aged subjects: an fMRI study. *Cerebral cortex (New York, N.Y. : 1991)*, *17*(10), 2453–2467. doi:10.1093/cercor/bhl153

Vogel, J. W., Joie, R. L., Grothe, M. J., Diaz-Papkovich, A., Doyle, A., Vachon-Presseau, E., … Evans, A. C. (2019). A molecular gradient along the longitudinal axis of the human hippocampus informs large-scale behavioral systems. doi: 10.1101/587071

Wechsler, D. (1987).Manual for the Wechsler Memory Scale-Revised, *The Psychological Corporation, San Antonio, TX.*

Weiner, M. W., Aisen, P. S., Jack, C. R., Jagust, W. J., Trojanowski, J. Q., Shaw, L., … Schmidt, M. (2010). The Alzheimer's Disease Neuroimaging Initiative: Progress report and future plans*. Alzheimer's & Dementia, 6(3), 202–211.e7.* doi:10.1016/j.jalz.2010.03.007

Weiner, M. W., Veitch, D. P., Aisen, P. S., Beckett, L. A., Cairns, N. J., Green, R. C., … Trojanowski, J. Q. (2013). The Alzheimer's Disease Neuroimaging Initiative: A review of papers published since its inception*. Alzheimer's & Dementia, 9(5), e111–e194.* doi:10.1016/j.jalz.2013.05.1769

Whitwell, J. L. (2009). Voxel-Based Morphometry: An Automated Technique for Assessing Structural Changes in the Brain*. Journal of Neuroscience, 29(31), 9661–9664.* doi:10.1523/jneurosci.2160-09.2009

Williams, M. M., Roe, C. M., & Morris, J. C. (2009). Stability of the Clinical Dementia Rating, 1979-2007*. Archives of Neurology, 66(6).* doi:10.1001/archneurol.2009.69

Williams, M. M., Storandt, M., Roe, C. M., & Morris, J. C. (2013). Progression of Alzheimer's disease as measured by Clinical Dementia Rating Sum of Boxes scores*. Alzheimer's & Dementia, 9(1), S39–S44.* doi:10.1016/j.jalz.2012.01.005

Woolrich, M. W., Jbabdi, S., Patenaude, B., Chappell, M., Makni, S., Behrens, T., … Smith, S. M. (2009). Bayesian analysis of neuroimaging data in FSL. NeuroImage, 45(1), S173–S186. doi:10.1016/j.neuroimage.2008.10.055

Wright, I. C., Ellison, Z. R., Sharma, T., Friston, K. J., Murray, R. M., & McGuire, P. K. (1999). Mapping of grey matter changes in schizophrenia. *This work was presented, in part, at the VIth International Congress on Schizophrenia Research, Colorado Springs, Colorado, USA, April 1997.1. Schizophrenia Research, 35(1), 1–14.* doi:10.1016/s0920-9964(98)00094-2

Wright, I. C., McGuire, P. K., Poline, J.B., Travere, J. M., Murray, R. M., Frith, C. D., … Friston, K. J. (1995). A Voxel-Based Method for the Statistical Analysis of Gray and White Matter Density Applied to Schizophrenia. *NeuroImage, 2(4), 244–252.* doi:10.1006/nimg.1995.1032

Zarei, M., Beckmann, C. F., Binnewijzend, M. A. A., Schoonheim, M. M., Oghabian, M. A., Sanz-Arigita, E. J., … Barkhof, F. (2013). Functional segmentation of the hippocampus in the healthy human brain and in Alzheimer's disease. *NeuroImage, 66, 28–35.* doi:10.1016/j.neuroimage.2012.10.071

Zilles, K., Schleicher, A., Palomero-Gallagher, N., & Amunts, K. (2002). Quantitative Analysis of Cyto- and Receptor Architecture of the Human Brain. *Brain Mapping: The Methods, 573–602.* doi:10.1016/b978-012693019-1/50023-x

Zhao, W., Wang, X., Yin, C., He, M., Li, S., & Han, Y. (2019). Trajectories of the Hippocampal Subfields Atrophy in the Alzheimer's Disease: A Structural Imaging Study. *Frontiers in Neuroinformatics,13*. doi:10.3389/fninf.2019.00013

Zola-Morgan, S., Squire, L., & Amaral, D. (1986). Human amnesia and the medial temporal region: enduring memory impairment following a bilateral lesion limited to field CA1 of the hippocampus. *The Journal of Neuroscience, 6(10), 2950–2967.* doi:10.1523/jneurosci.06-10-02950.1986